European Journal of Medicinal Chemistry 229 (2022) 114097

Contents lists available at ScienceDirect

European Journal of Medicinal Chemistry

journal homepage: http://www.elsevier.com/locate/ejmech

Synthesis of novel thiazolyl hydrazone derivatives as potent dual monoamine oxidase-aromatase inhibitors

Asaf Evrim Evren [a, b, *], Demokrat Nuha [a, c], Sam Dawbaa [a, d], Begüm Nurpelin Sağlık [a], Leyla Yurttaş [a]

[a] Anadolu University, Faculty of Pharmacy, Department of Pharmaceutical Chemistry, 26470, Eskişehir, Turkey
[b] Bilecik Şeyh Edebali University, Vocational School of Health Services, Department of Pharmacy Services, 11000, Bilecik, Turkey
[c] Eskisehir Technical University, Faculty of Science, Department of Chemistry, 26555, Eskişehir, Turkey
[d] Department of Pharmacy, Faculty of Medicine and Health Sciences, Thamar University, Dhamar, Yemen

ARTICLE INFO

Article history:
Received 31 October 2021
Received in revised form
20 December 2021
Accepted 29 December 2021
Available online 1 January 2022

Keywords:
2-Thiazolylhydrazones
Monoamine oxidase inhibition
Aromatase inhibition
Molecular docking
Molecular dynamic simulation
QSAR

ABSTRACT

The inhibitory effects of 2-thiazolyl hydrazones on monoamine oxidase enzymes are known for a long time. In this study, a new series of 2-thiazolyl hydrazone derivatives were synthesized starting from 6-methoxy-2-naphthaldehyde. All of the synthesized compounds were investigated in terms of their monoamine oxidase (MAO) inhibitory effects and significant results were found. The results showed that compound **2j** potently inhibited MAO-A and MAO-B, while compound **2t** strongly and selectively inhibited MAO-B compared to standard drugs. Compounds **2k** and **2q** exhibited selective and satisfying inhibition on MAO-B. In the aromatase inhibition studies of the compounds, it was determined that compounds **2q** and **2u** had high inhibitory properties. Molecular docking studies on MAO-A, MAO-B, and aromatase enzymes were carried out for the aforementioned compounds. Additionally, molecular dynamics simulation was studied for compound **2q** on MAO-B and aromatase complexes. Finally, the Field-based QSAR study was developed and the structure-activity relationship (SAR) was explained. For the first time, dual inhibitors on MAO and aromatase enzyme were investigated together. The aim of this approach is for finding the potential agents that do not cause the cognitive disorders and may even treat neurodegenerative symptoms, thus, the aim was reached successfully.

1. Introduction

Monoamine oxidases (MAO) are mitochondrial flavoenzymes consisting of two isoforms (MAO-A and MAO-B) according to their distribution in tissues, substrate and inhibitor specificity, and immunological properties. They are mostly found in gastrointestinal, hepatic, and neuronal tissues and catalyze the oxidative deamination of endogenous and exogenous amines (dopamine, noradrenaline). In the central and peripheral nervous system, MAO catalyzes the metabolic conversion of amine neurotransmitters, while in the liver, MAO acts as a detoxifying enzyme against foreign amine compounds entering the body [1,2]. As a drug, monoamine oxidases inhibitors show their effects in psychiatric (depression) and neurological disorders (Parkinson's disease, PD) by increasing the neurotransmitter levels in the relevant tissues [3,4]. Increasing norepinephrine levels (as well as dopamine and serotonin concentrations) with MAO-A inhibitors such as tranylcypromine is the mainstay of treatment for depression. Recently, although selective serotonin reuptake inhibitors (SSRIs) and tricyclic antidepressants have been used more frequently in the treatment of depression, there may be cases or patients in which MAO-A inhibitors are superior [5]. MAO-B inhibitors, on the other hand, have a higher affinity for phenylethylamine and benzylamine and can prevent dopamine deficit caused by an increase in MAO-B expression in the brain due to aging, as well as the progression of PD [6].

2-Thiazolylhydrazones are remarkable compounds that were reported to have monoamine oxidase inhibition activity. Chimenti and his study group synthesized a large number of thiazolylhydrazine compounds which include various aromatic rings, aliphatic cyclic rings and groups, and evaluated their MAO inhibition activities [7–9]. They observed high activity in many

* Corresponding author. Anadolu University, Faculty of Pharmacy, Department of Pharmaceutical Chemistry, 26470, Eskişehir, Turkey.,
E-mail addresses: asafevrimevren@anadolu.edu.tr, asafevrim.evren@bilecik.edu.tr (A.E. Evren).

https://doi.org/10.1016/j.ejmech.2021.114097
0223-5234/

compounds and described 4-aryl-2-thiazolylhydrazone moiety as a pharmacophore for MAO inhibition. They observed high and selective inhibition of MAO-B (at nM concentration) as well as high inhibition of MAO-A in compounds containing the scaffold that had various cycloaliphatic rings attached to the azomethine carbon and 4-aryl thiazoles substituted with NO_2 and F groups. According to their QSAR study, MAO inhibitors should contain a basic nitrogen atom and an electron-rich aromatic ring (Fig. 1) [10]. Another study reported that MAO-A inhibition, particularly inhibition of MAO-B, was observed in compounds derived from various heteroaromatic ketones and aldehydes. These derivatives were able to inhibit *h*MAO-B at micromolar to nanomolar concentration. The best inhibitory activity was observed by the derivatives that contain pyridine as the heterocyclic ring [11]. In another study, excellent and selective inhibition of MAO-B was observed in derivatives obtained from 3- and 4-pyridine carboxaldehyde and phenyl and -COOEt bonded to the 4th position of a thiazole ring (Fig. 1).

For selectivity, electron-rich aromatic ring for MAO-A inhibition, lipophilicity for MAO-B inhibition are considerable criteria while the interaction of the amino acids Tyr326 and Ile335 in the active site of the enzyme enhances the selectivity for MAO-A and MAO-B, respectively [12]. Moreover, 3-nitrophenyl-containing molecules at C_4 of the thiazole ring with various heteroaromatic rings bonded to azomethine carbon were characterized with high anti-MAO-B activity [13]. Similarly, in many different studies, thiazolyl hydrazones were evaluated in terms of MAO inhibition and reproducible high-activity results were obtained [14–16]. Furthermore, several of the newly synthesized aromatic ring-containing compounds were discovered to have active molecules at the micromolar level that were neither cytotoxic nor genotoxic [17].

Estradiol, the most potent endogenous estrogen, is biosynthesized from androgens by the cytochrome P450 enzyme complex, called aromatase. Breast tissue normally contains aromatase, and intratumoral aromatase produced in breast cancer tissues is a local source of estrogen. Aromatase inhibition is an important approach used to reduce the growth stimulant in cases of estrogen-dependent breast cancer. Aromatase inhibitors (AIs) are among the drug groups used in the treatment of breast cancer, and the development of drug resistance is a challenging issue in treatment. It is used alone or in combination with other agents, based on data from clinical studies [18,19]. The steroidal aromatase inhibitors bind to the enzyme irreversibly while nonsteroidal inhibitors bind to it reversibly. Nonsteroidal aromatase inhibitors can be divided into three classes: azoles, stilbene derivatives, and flavonoid analogues [20,21]. Among them, it is known that azoles including thiazole, oxadiazole, and tetrazole rings are preferable synthetic structures for aromatase inhibition. The suitable heteroatoms of these molecules form chelates by coordinating with the iron in the HEM structure of the aromatase enzyme and, as a result, aromatization is inhibited and the pathological biosynthetic pathway leading to tumorigenesis is disrupted [22]. On the other hand, several studies have been published that include bicyclic rings such as naphthalene, coumarin, quinoline, and isoquinoline, because of their inhibition ability related to the steroidal cancer pathways [23–29]. Additionally, the effect of numerous thiazole derivatives on breast cancer was studied focusing on aromatase inhibition [30–33]. In a recent study, chlorophenyl containing 2-thiazolyl hydrazones exhibited high aromatase inhibitory activity [34].

Moreover, aromatase amounts are particularly high in temporal and frontal brain areas; as known, these regions are generally associated with learning, memory, and sensory processing (temporal lobes) and dopaminergic activity (frontal lobes) in the human brain. On the other hand, using aromatase inhibitors in cancer treatments such as breast cancer, caused cognitive disorders in these patients and it is among the important side effects [35]. To eliminate or at least reduce such neurological side effects, focusing on inhibition of both MAO and aromatase (Cyp19 gene) enzymes may be a new treatment approach. Thus, it takes priority to evaluate current MAO inhibitors against aromatase or to find new inhibitors which inhibit both enzymes. In our study, we designed the hybridization of both cores as shown in Fig. 1.

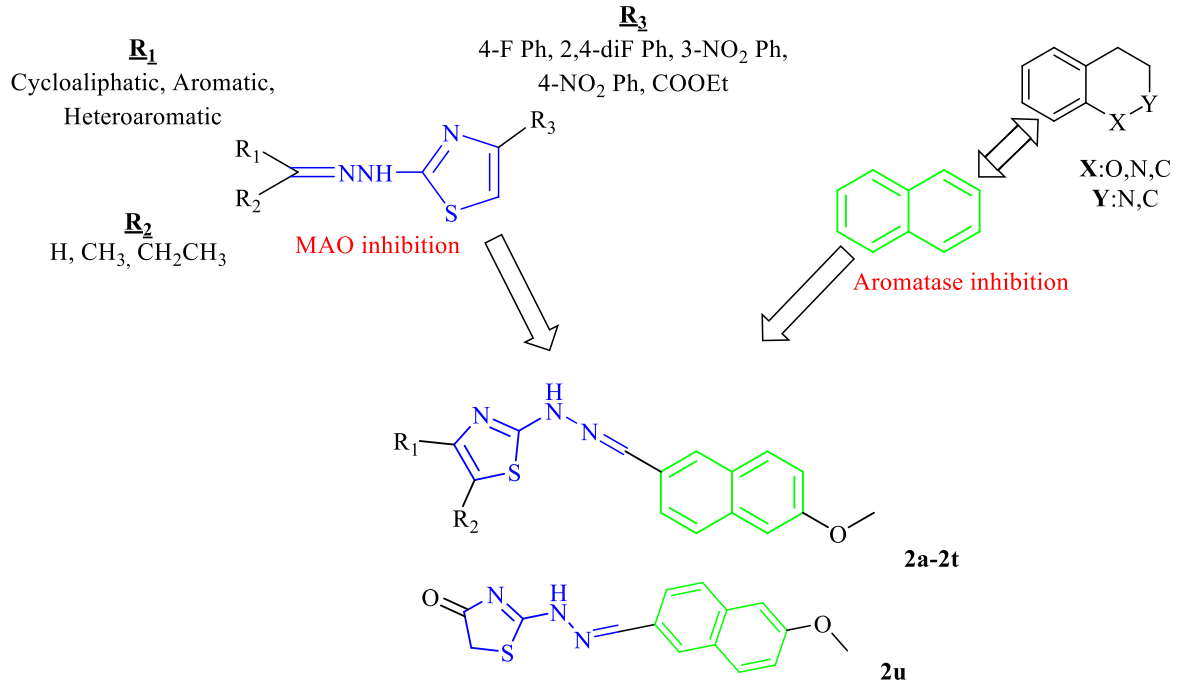

Fig. 1. Designing approach to the goal molecules.

Accordingly, a new series of 2-thiazolylhydrazone derivatives containing 6-methoxynaphthalene ring were synthesized, in this study. The compounds were tested for inhibiting MAO-A, MAO-B, and aromatase enzymes and the results were evaluated in light of literature data.

2. Results and discussion

2.1. Chemistry

The target products were recrystallized from ethanol. Purity determination and structure elucidation were achieved by melting point analysis, Proton Nuclear Magnetic Resonance (^{1}H NMR) spectrometry, Carbon Nuclear Magnetic Resonance (^{13}C NMR) spectrometry, elemental analysis, and high-resolution mass spectrometry (HRMS). The results are shown in Figs. S1−S63.

^{1}H NMR spectra of the products were obtained in 300 MHz instrument. Aromatic methyl groups in general were observed in a range of chemical shifts of 2.30−2.50 ppm. Aliphatic methyl's peak was seen between 1.20 and 1.30 ppm like that of **2q**, where it occurred in 1.21 ppm while that of **2s** appeared in 1.27 ppm. Methyl group bound to sulphonyl in compound **2l** was shifted to the downfield by the effect of the sulphonyl group and has a chemical shift of 3.24 ppm. Hydrogens bound to carbon number 5 of thiazol-4(5*H*)-one of compound **2u** were shown as a singlet and the compound's NMR spectrum was a proof for the formation of the oxo group at position 4. Hydrogens of esteric methylene of compounds **2q** and **2s** were observed in 4.12 and 4.21 ppm respectively while those of methylene of −CH_2COO- in compound **2q** were observed in 3.74 ppm. Singlet peak of the hydrogens of −OCH_3 in naphthalene's 6th position occurs at 3.89 ppm in all compounds. The aromatic region between 6.5 and 8.5 ppm shows a complex pattern of peaks. Hydrogen at 7th position of naphthalene resonates at 7.20 (some compounds at 7.19) ppm and appears as a doublet of doublets (dd) peak. Similarly, 6-H of naphthalene resonates as a doublet (d) at 7.35 (or 7.36) ppm. Hydrogen in H−C═N occurred between 8.15 and 8.20 ppm except for compounds **2q** and **2s** where it was observed at 8.37 and 8.01 ppm, respectively. The broad singlet peaks around 12 ppm represent N−H hydrogen.

In ^{13}C NMR spectra, methoxy group signals appeared between 55.50 and 55.82 ppm. −CN group bound to the phenyl ring in compound **2i** has a signal at 109 ppm. Alkyl substituents such as methyl had signals in the aliphatic region less than 100 ppm as expected and the chemical shifts differ according to the site of the group. The aromatic region of the spectra between 100 and 180 ppm showed a crowd of signals as the biggest parts of the compounds are aromatic rings. The signal of carbon in H−C═N kept at appearing around 142 ppm. The ester carbonyl of compound **2s** showed a signal at 180.94 ppm. Signal at 174.65 ppm of compound **2u** belongs to the carbonyl of thiazol-4(5H)-one. HRMS and elemental analyses confirmed the structural backbone of the compounds as shown in the analytical monographs.

2.2. ADME parameters

Using the SwissADME web tool, an *in silico* ADME (Absorption, Distribution, Metabolism, and Excretion) study of compounds **2a-2u** and standard drugs were done, and essential five physicochemical parameters were determined [36,37]. The values of hydrogen bond-acceptors (HBA), hydrogen bond-donors (HBD), topological polar surface area (TPSA), lipophilicity descriptor (Log P), water solubility descriptor (Log S), skin permeation descriptor (Log K), gastrointestinal absorption (GIA), and other parameters are depicted in Table S1. Based on Lipinski "Rule of 5", all the prepared compounds have good membrane permeability (BBB/GI), log P (3.66−5.98) ≤6, number of hydrogen bond acceptors (3−5) ≤10, molecular weight ≤500, and the number of hydrogen bond donor (1) ≤5 [38,39]. The pharmacophore or drug-like qualities of the compounds revealed that they all follow and satisfy the Lipinski's rule, with all features falling within a reasonable range [40]. These scores are in line with the activity potential of those compounds. It is thought that the synthesized compounds might have a good pharmacokinetic profile. Thus, the drug-likeness of the compounds was dedicated positive.

2.3. Results of in-vitro enzyme studies

Twenty-one thiazole derivatives bearing 6-methoxynaphthalene were synthesized and the monoamine oxidase A and B inhibition activities of these compounds at 10^{-3} and 10^{-4} M concentrations were evaluated. The percent inhibitions of the compounds on these enzymes are given in Table 1 with the standard drugs moclobemide and selegiline.

The compounds **2j** and **2t**, which provide more than 50% inhibition on MAO-A at 10^{-4} M concentration, and compounds **2j, 2k,** and **2q**, which provide more than 50% inhibition on MAO-B, were tested at lower concentrations to determine IC_{50} concentrations. The determined IC_{50} concentrations of these compounds are shown in Table 2.

Among the compounds, **2j**, which carries 3-nitrophenyl on the thiazole ring, and **2t**, which carries phenyl and methyl in the thiazole, exhibited 84.13% and 82.31% percent inhibition over MAO-A at 10^{-4} concentration, respectively, and this rate is slightly higher than the percentage of moclobemide (82.14%). In addition, the IC_{50} values of these compounds which were 0.068 μM for **2j** and 0.072 μM for **2t** are significantly lower than that of the standard drug. The compounds **2j** showed 89.10%, **2k** 85.24%, and **2q** showed 90.04% inhibition which were slightly lower than the standard drug against the MAO-B enzyme, at a concentration of 10^{-4}. Among these compounds, **2q**, which carries ethoxyacetyl on thiazole, was found to be the closest potential to selegiline (IC_{50}:0.036 μM) with an IC_{50} value of 0.039 μM. This value was determined as 0.082 μM and 0.046 μM for **2j** and **2k,** respectively.

In this study, the aromatase enzyme inhibition of the compounds was also studied. All of the compounds were evaluated with a pre-docking study in the Schrödinger Maestro program, according to which compounds that could show potential inhibition, **2q** and **2u**, were tested on the aromatase enzyme. Accordingly, the IC_{50} values of these compounds were determined as 0.031 μM and 0.042 μM, respectively. The IC_{50} value of the standard drug letrazole was determined as 0.026 μM. The results are presented in Table 2.

2.4. Results of molecular docking studies

SAR studies are useful and very important to explain the activity of the compounds, and/or design new compounds, and/or eliminate or clarify the adverse effects of current agents. There are numerous ways to achieve that. One of them is the computer-aided studies which are applicable easily on a wide range, and very harmless methods when compared with *in-vitro* and *in-vivo* studies. For that, on the active molecules, we first did molecular docking and subsequently molecular dynamic simulation investigations. At this process, these compounds were examined for their binding mode at the active region of the related protein.

2.4.1. Docking study on MAO-A enzyme

Since the IC_{50} values of **2j** and **2t** are very close to each other, they were considered for the docking study. The 3D poses obtained from docking studies were shown in Figs. 2 and 3, and the 2D poses

Table 1
Inhibition% of the synthesized compounds, moclobemide and selegiline against MAO-A and MAO-B.

Compounds	MAO-A % Inhibition		MAO-B % Inhibition	
	10^{-3} M	10^{-4} M	10^{-3} M	10^{-4} M
2a	51.445 ± 0.895	26.637 ± 0.798	72.365 ± 0.985	42.927 ± 0.832
2b	49.835 ± 0.982	31.126 ± 0.932	77.895 ± 1.130	43.436 ± 0.951
2c	56.685 ± 1.028	21.863 ± 0.884	68.934 ± 1.348	42.002 ± 0.958
2d	50.002 ± 0.926	28.084 ± 0.861	79.714 ± 1.045	39.647 ± 0.902
2e	48.447 ± 0.724	39.920 ± 0.727	71.026 ± 1.162	47.285 ± 0.874
2f	48.351 ± 0.962	28.848 ± 0.862	68.532 ± 1.091	41.761 ± 0.990
2g	59.402 ± 0.931	32.147 ± 0.825	75.478 ± 1.075	40.715 ± 0.851
2h	52.165 ± 0.945	35.465 ± 0.744	65.151 ± 0.927	46.252 ± 0.848
2i	58.698 ± 0.985	30.448 ± 0.812	76.278 ± 1.202	40.391 ± 0.764
2j	90.525 ± 1.028	84.133 ± 1.247	94.274 ± 1.033	89.102 ± 1.005
2k	57.788 ± 0.837	33.391 ± 0.857	89.377 ± 1.152	85.241 ± 1.233
2l	53.497 ± 0.848	37.013 ± 0.847	73.463 ± 1.434	46.425 ± 0.995
2m	59.202 ± 0.802	34.197 ± 0.899	79.502 ± 1.162	44.191 ± 0.848
2n	55.854 ± 1.146	35.696 ± 0.897	70.299 ± 1.126	45.834 ± 0.993
2o	47.686 ± 0.907	32.458 ± 0.791	76.351 ± 1.230	38.262 ± 0.758
2p	58.443 ± 0.894	27.746 ± 0.735	71.520 ± 1.002	43.120 ± 0.916
2q	60.245 ± 0.902	30.228 ± 0.862	96.487 ± 1.123	90.035 ± 1.298
2r	54.388 ± 0.932	30.920 ± 0.784	68.385 ± 1.315	43.063 ± 0.833
2s	58.168 ± 0.864	29.316 ± 0.702	68.936 ± 1.247	41.885 ± 0.854
2t	90.918 ± 1.145	82.321 ± 1.065	79.048 ± 1.348	46.674 ± 1.074
2u	55.817 ± 0.948	33.880 ± 0.641	66.154 ± 1.195	47.974 ± 0.920
Moclobemide	94.121 ± 2.760	82.143 ± 2.691	–	–
Selegiline	–	–	99.387 ± 1.385	95.629 ± 1.456

Table 2
IC_{50} values of compounds **2j, 2k, 2q, 2t, 2u,** moclobemide, selegiline and letrazole against MAO-A, MAO-B, and aromatase enzymes.

Compounds	IC_{50} (μM)		
	MAO-A	MAO-B	Aromatase
2j	0.068 ± 0.002	0.046 ± 0.002	–
2k	–	0.082 ± 0.003	–
2t	0.072 ± 0.003	–	–
2q	–	0.039 ± 0.001	0.031 ± 0.001
2u	–	–	0.042 ± 0.001
Moclobemide	6.061 ± 0.262	–	–
Selegiline	–	0.036 ± 0.001	–
Letrazole	–	–	0.026 ± 0.001

were in Figs. S64–65.

Between compound **2j** and the protein, there were two hydrophobic (one π-cation and one π-π) interactions and 8 aromatic H-bonds (Fig. 2 and Fig. S64). π-cation interaction was observed between phenyl of Tyr444 and N^+ of nitro group of the ligand. π-π interaction was seen between phenyl of ligand and the phenyl of Tyr407. Aromatic H-bonds were between $C_5\underline{H}$ of naphthalene ring of **2j** and the carbonyl oxygen of Phe208; $C_8\underline{H}$ of naphthalene ring of **2j** and the carbonyl oxygen of Tyr306; $C_5\underline{H}$ of thiazole ring of **2j** and the carbonyl oxygen of FAD protein; $C_4\underline{H}$ of the phenyl ring of **2j** and the carbonyl oxygen of Asn181 and also methoxy oxygen of Tyr197; $C_5\underline{H}$ of the phenyl ring of **2j** and the carbonyl oxygen of Asn181 and also amidic oxygen of Asn181.

Between compound **2t** and the protein, there were 4 π-π interactions and 4 aromatic H-bonds (Fig. 3 and Fig. S65). The phenyl ring of **2t** interacted with the phenyl ring of Tyr407 and the phenyl ring of Tyr444. Also, thiazole ring of **2t** and phenyl ring of Tyr407 interacted via π-π. On the contrary to **2j**, between the naphthalene ring of **2t** and phenyl ring Phe208 was shown π-π interaction. Aromatic H-bonds were seen between $C_7\underline{H}$ of naphthalene ring of **2t** and the carbonyl oxygen of Ala111; $C_4\underline{H}$ of the phenyl ring of **2t** and the carbonyl oxygen of Asn181 and also methoxy oxygen of Tyr197; $C_5\underline{H}$ of the phenyl ring of **2t** and the carbonyl oxygen of Asn181 and also amidic oxygen of Asn181.

According to docking studies, these two compounds (**2j** and **2t**) fit well into the binding region, and also had interactions with significant residues for MAO-A inhibition activity. In conclusion, the results obtained from docking studies were in harmony with the results of the *in-vitro* enzyme study.

2.4.2. Docking study on MAO-B enzyme

The most active compounds were determined as **2j, 2k,** and **2q**. The 3D poses obtained from docking studies were shown in Figs. 4–6, and the 2D poses were in Figs. S66–68.

Between compound **2k** and the MAO-B enzyme, there were 2 π-π interactions and 4 aromatic H-bonds (Fig. 4 and Fig. S66). The thiazole ring of **2k** interacted with the phenyl ring of Tyr326. Also, naphthalene ring of **2k** and phenyl ring of Tyr398 interacted via π-π. Aromatic H-bonds were seen between $C_2\underline{H}$ and $C_3\underline{H}$ of phenyl ring of **2k** and the methoxy oxygen of Tyr326; $C_3\underline{H}$ of the naphthalene ring of **2k** and the amidic oxygen of Gln206; $C_8\underline{H}$ of the naphthalene ring of **2k** and the N_5 of FAD protein.

At the active site of MAO-B, compound **2j** displayed 3 π-π interactions and 5 aromatic H-bonds (Fig. 5 and Fig. S67). The π-π interactions were the same as the relations between **2k** and Tyr326, **2k** and Tyr398, but in addition to these, there was also between the naphthalene ring of **2j** and the phenyl ring of Phe343. Aromatic H-bonds were observed between $C_4\underline{H}$ of the naphthalene of **2j** and the oxygen of FAD protein; oxygen of nitro group of **2j** and $C_6\underline{H}$ of indole of Trp116; $C_4\underline{H}$ of phenyl of **2j** and carbonyl oxygen of Pro102; $C_4\underline{H}$ of phenyl of **2j** and carbonyl oxygen of Ile199 and also methoxy oxygen of Tyr326.

There were observed 2 π-π interactions, one H-bond and 3 aromatic H-bonds between **2q** and MAO-B enzyme (Fig. 6 and Fig. S68). Although the π-π interactions were similar to **2k** or **2j**, this time, thiazole of ligand posed interaction with Tyr398 and naphthalene of ligand with Tyr326. A H-bond was formed between thiazole nitrogen of **2q** and Gln206. Aromatic H-bonds were observed between $C_5\underline{H}$ of the naphthalene ring of **2q** and methoxy oxygen of Tyr326; $C_5\underline{H}$ of thiazole of **2q** and phenyl of Tyr398; carbonyl oxygen of **2q** and C3H of phenyl of Tyr435.

According to the docking studies, both *in-vitro* and *in-silico* studies revealed that **2q** fitted well into the binding region and had

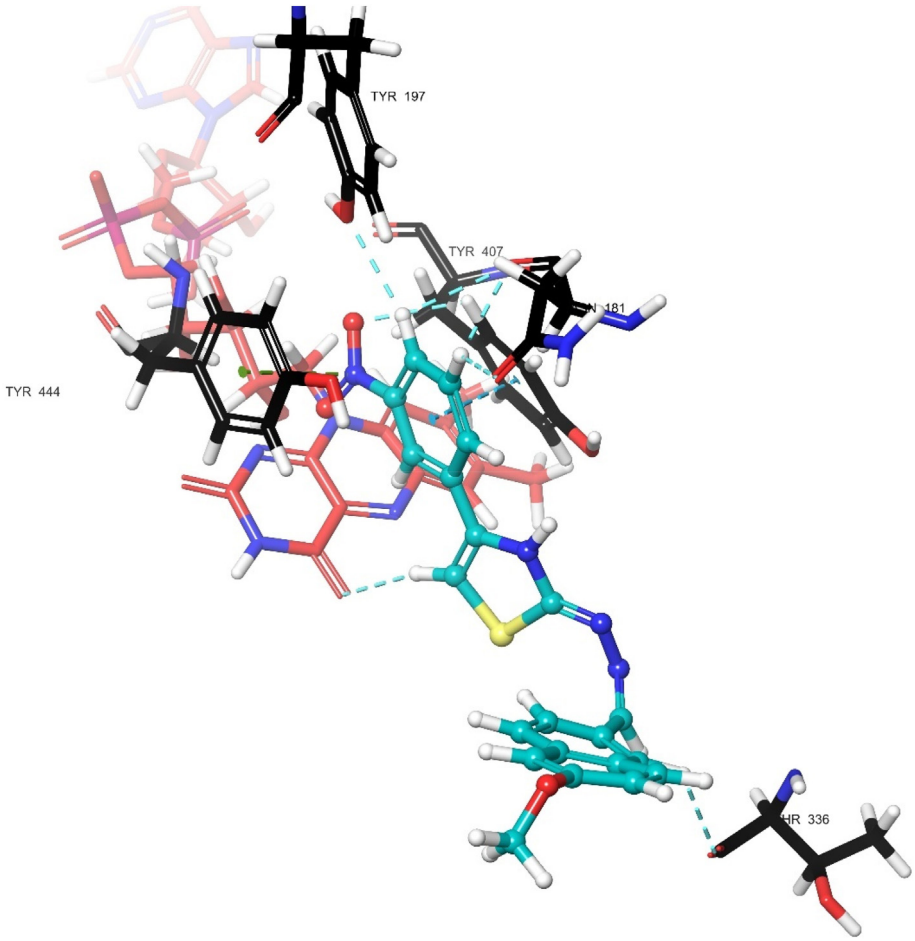

Fig. 2. The aspect of **2j**-MAO-A enzyme complex as 3D (PDBID: 2Z5X).

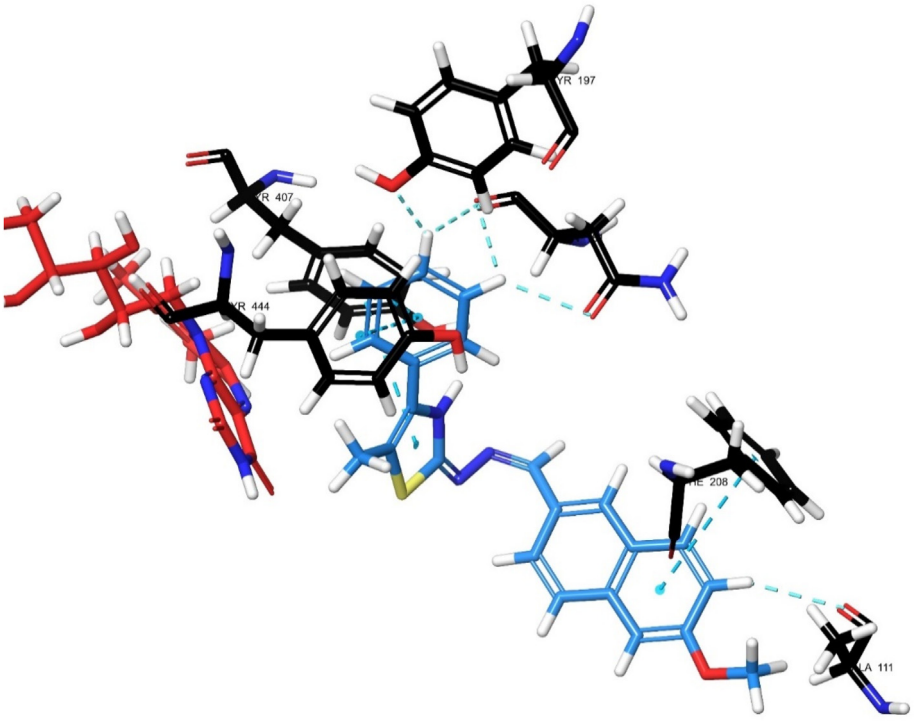

Fig. 3. The aspect of **2t**-MAO-A enzyme complex as 3D (PDBID: 2Z5X).

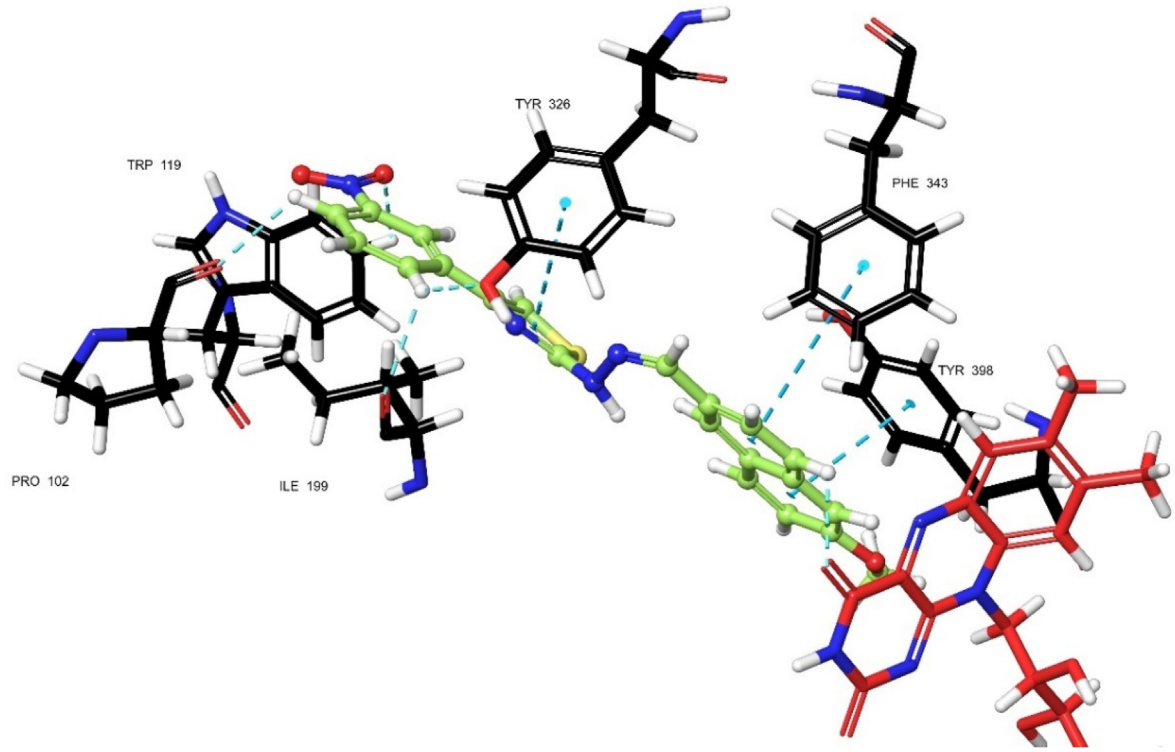

Fig. 4. The aspect of **2j**-MAO-B enzyme complex as 3D (PDBID: 2V5Z).

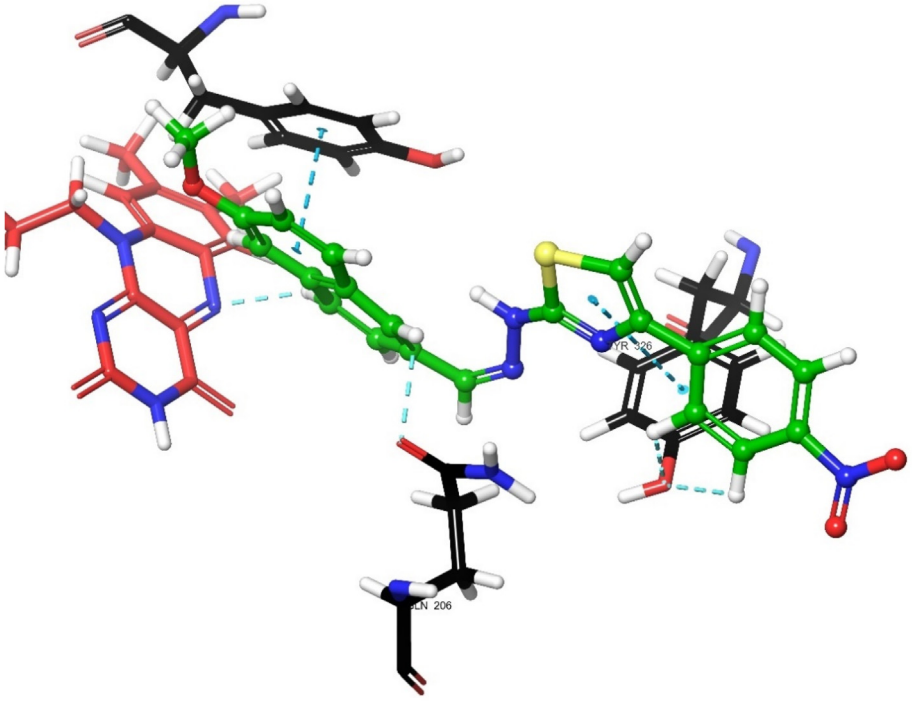

Fig. 5. The aspect of **2k**-MAO-B enzyme complex as 3D (PDBID: 2V5Z).

interactions with significant residues for MAO-B inhibition activity. Also, compounds **2k** and **2q** interacted with Gln206, which was an important residue for the MAO-B selectivity. In conclusion, the results obtained from the docking studies were in harmony with the results of *in-vitro* enzyme studies.

2.4.3. Docking study on aromatase enzyme

The most active compounds were determined as **2q** and **2u** against aromatase enzyme. The 3D poses obtained from the docking studies are shown in Figs. 7 and 8, and the 2D poses are in Figs. S69–70.

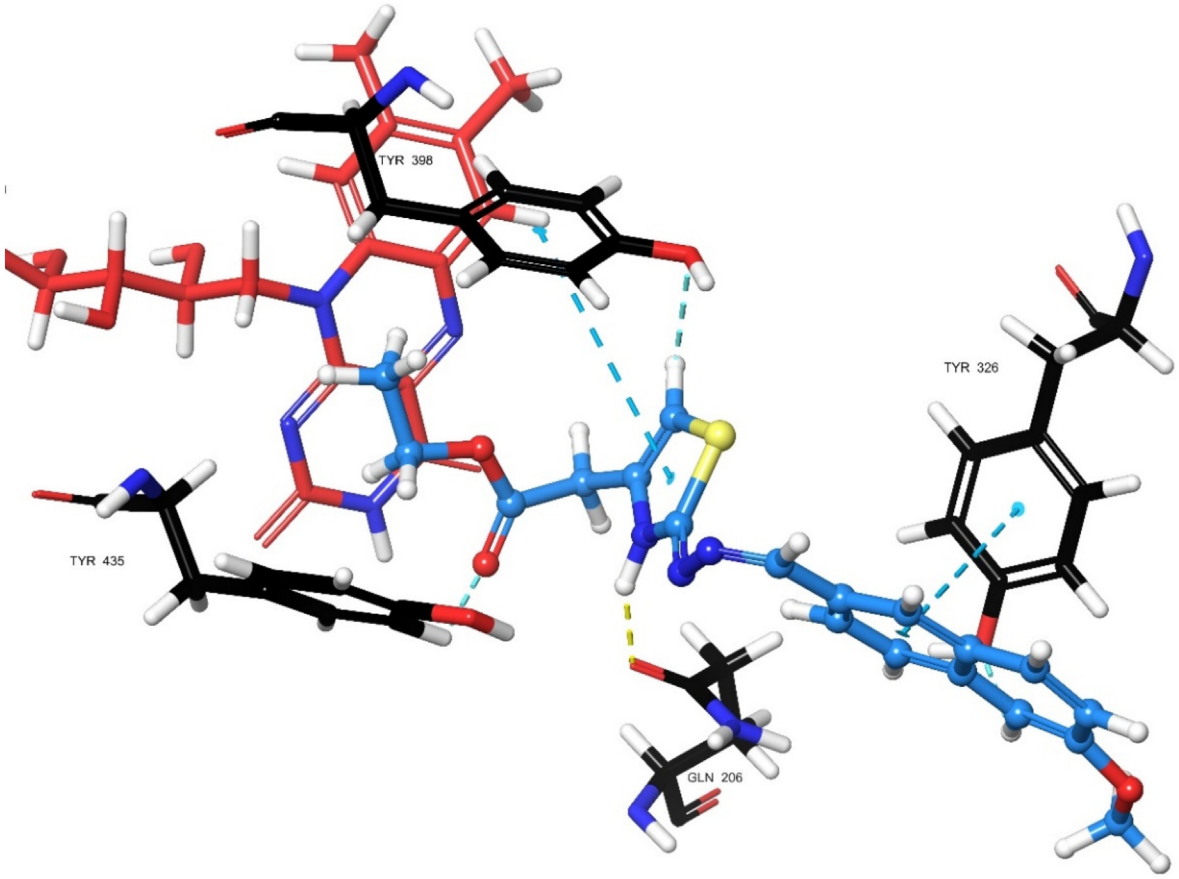

Fig. 6. The aspect of **2q**-MAO-B enzyme complex as 3D (PDBID: 2V5Z).

The docking study of the active compounds **2q** and **2u** with the aromatase enzyme depicted that the compounds formed π-π interactions with the HEM group (Figs. 7 and 8). Also, there were 2 H-bonds, and 2 aromatic H-bonds for **2q**. H-bonds were observed between hydrazone of **2q** and hydroxyl group of Tyr310; methoxy group of **2q** and amine group of Met374. Aromatic H-bonds were between C_7H of naphthalene of **2q** and carbonyl group of Leu372; ethoxy oxygen of **2q** and C_6H of the indole ring of Trp224.

Besides that, there were 3 aromatic H-bonds between **2u** and the protein. These were methoxy oxygen of **2u** and hydroxy of Thr310; hydrazone of **2u** and Met374; thiazole nitrogen of **2u** and carbonyl group of Leu372.

According to docking studies, both *in-vitro* and *in-silico* studies showed that **2q** and **2u** fitted well into the binding region, and also made interactions with significant residues for the enzyme activity. In conclusion, the results obtained from the docking studies were in harmony with the results of *in-vitro* enzyme studies.

2.5. Results of molecular dynamic simulation (MDS) studies

2q was found as a significantly important analog due to its aromatase and selective MAO-B inhibition activities, thus, the MDS study was separately performed for **2q**-enzyme complexes. MDS studies were performed based on the best docking poses. Moreover, the ligand-enzyme stability during the entire simulation is an important issue because of the continuity of the interactions, thus, values of root mean square deviation (RMSD), root mean square fluctuation (RMSF), and the radius of gyration (Rg) are good guides for the researchers to understand this issue.

2.5.1. MDS on 2q and MAO-B complex

Data obtained from MDS were displayed in Fig. S71 and Fig. 9. Fig. S71 demonstrated that the ligand-enzyme complex is stable. Protein and/or complex compactness are denoted by Rg, in this case, the Rg plot has represented the stability was under control between 10 and 47.5 ns. RMSD value of protein was calculated between 1 and 3 Å during the entire simulation, which is indicative of stability for small proteins [41]. The α-helix (red areas) and the β-strand (blue areas) have usually minimum fluctuation. Besides that, although the loop (white area) region may show big fluctuation [42], in this simulation, there are no high-low picks. Therefore, the RMSF result is a shred of significant evidence that the high stability of the complex during the simulation.

In Figs. 9 and 2q and interacting residues were redescribed in different ways. The π-π interactions were formed with Tyr60, Leu88, Phe99, Phe168, Leu171, Ile198, Ile199, Gln206, Tyr326, Leu328, Met341, Phe343, Tyr398, and Tyr435, the H-bond interactions were observed with Cys172, Gln206, Tyr326, and Tyr435. On the other hand, water-mediated H-bonds were seen between Glu101, Pro102, and Ile199. In addition to these, the ligand was perpetually in interaction with Tyr60, Leu171, Ile199, Ile316, Tyr326, and Tyr398 amino acids. Moreover, aromatic H-bonds were observed between 2q and Tyr60, Phe99, Pro102, Ile198, Ile199, Tyr326, Phe343, Tyr398, and Tyr435 amino acids and FAD protein (video-1, aromatic H-bond was represented as faded teal dashes, and other interaction types were hidden for clarity). MD simulation and the obtained docking pose were a good representation of each other. But, with the MDS study, the interaction between 2q and FAD protein was detectable and clarified the SAR of 2q. Consequently,

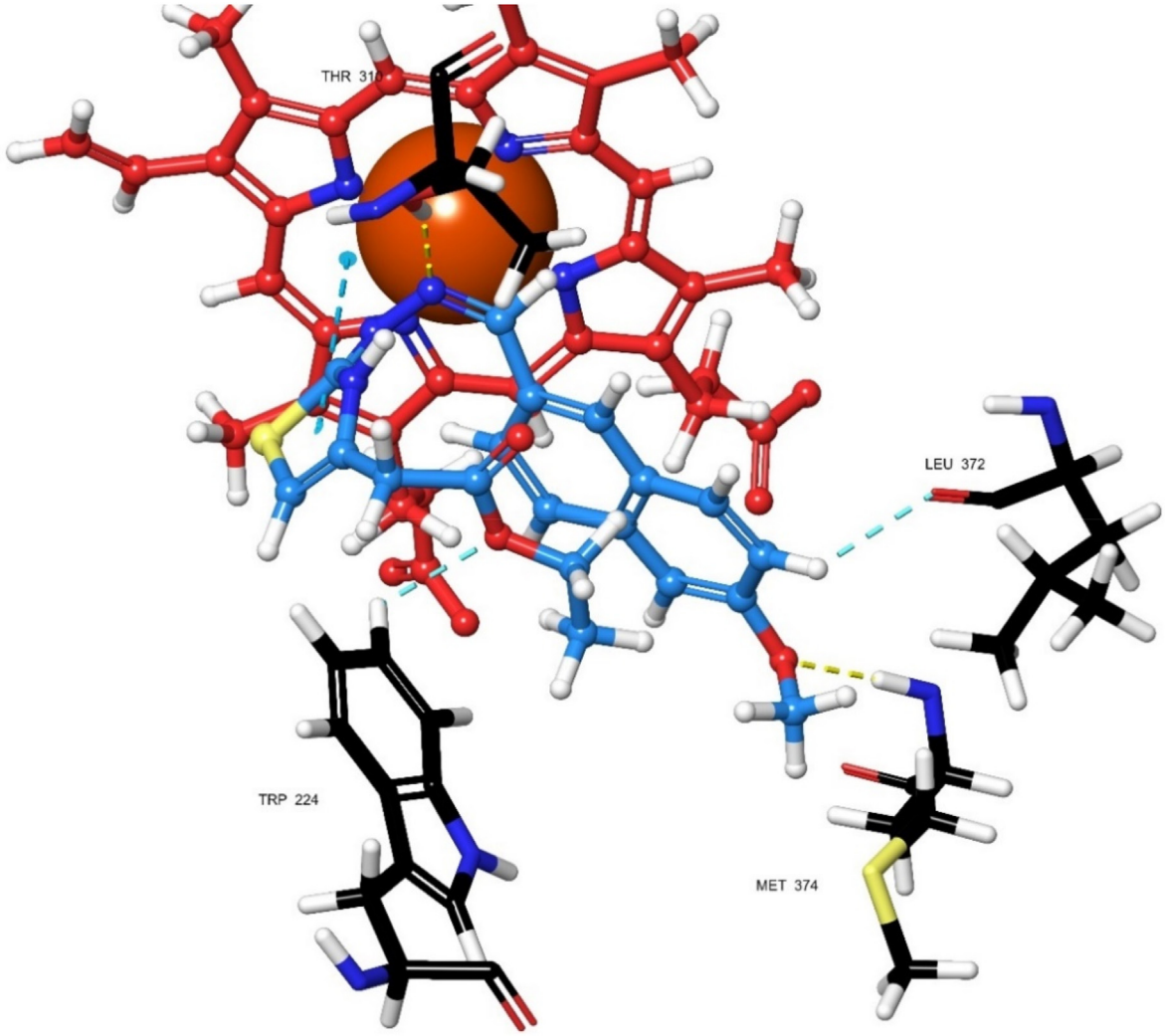

Fig. 7. The aspect of **2q**-Aromatase enzyme complex as 3D (PDBID: 3EQM).

since the ester group (carbonyl oxygen) and FAD protein (H_6) interacted frequently by aromatic H-bond, the polar group substitution at this position was found significant for the inhibitory activity.

2.5.2. MDS on 2q and aromatase complex

Data obtained from MDS were displayed in Fig. S72 and Fig. 10.

Fig. S72 showed that the 2q-aromatase enzyme complex was stable during the simulation. Moreover, same as Fig. S71, the Rg plot illustrated that the stability was under control during the entire simulation. RMSD value of protein was calculated between 1 and 3 Å during the entire simulation, similar to the 2q-MAO-B enzyme complex. The α-helix (red areas) and the β-strand (blue areas) have usually minimum fluctuation. The loop (white area) region had small fluctuation too, thus, the RMSF result is a shred of significant evidence of the high stability of the complex during the simulation.

In Figs. 10 and 2q and interacting residues were redescribed in different ways. The hydrophobic interactions were seen between 2q and Ile133, Phe134, Phe221, Trp224, Ile305, Ala306, Val313, Val370, Val373, Met374, and Leu477 amino acids. Additionally, H-bonds were formed with Gln225, Thr310, Met374, and Ser478. Also, water-mediated H-bonds were seen with Gln225, Val369, Asp371, Leu372, and Ser478. Moreover, the ligand intensively interacted with Ile133, Phe134, Phe221, Trp224, Thr310, Met374, and Ser478 amino acids. On the other hand, in video-2, only aromatic H-bonds and hydrophobic interactions with the HEM group were represented as faded teal dashes and blue dashes. The rest of the interaction types were hidden for clarity. Aromatic H-bonds were between 2q and Phe134, Phe221, Trp224, Leu372, and Ser478 amino acids. As seen in video-2, the number of interactions between 2q and HEM protein was changeable but it was continuous. As an important point, aromatic bicyclic scaffolds such as naphthalene are favorable due to potential pi-electron clouds, which interact with the HEM protein.

2.6. Validation of the FB-QSAR model and its results for MAO-B inhibition

The validation of the model was controlled via R^2, Q^2, Pearson-r, stability, RMSE, F and P values (Table 3). As mentioned in the related method section in this article, all the values and the relation between them were in an acceptable range. The model that has acceptable validation criteria thresholds for all conditions, is the final model that was used. This model is robust and able to make good internal and external predictions. In addition, this model can be a contributing tool for medicinal chemists to design new agents which are more effective and have fewer side effects.

The field-based QSAR (FB-QSAR) results are shown in Table 4. After the built-up of the QSAR model, active compound **2q** was modeled. Because factor 5 is the most ideal model than other PLS

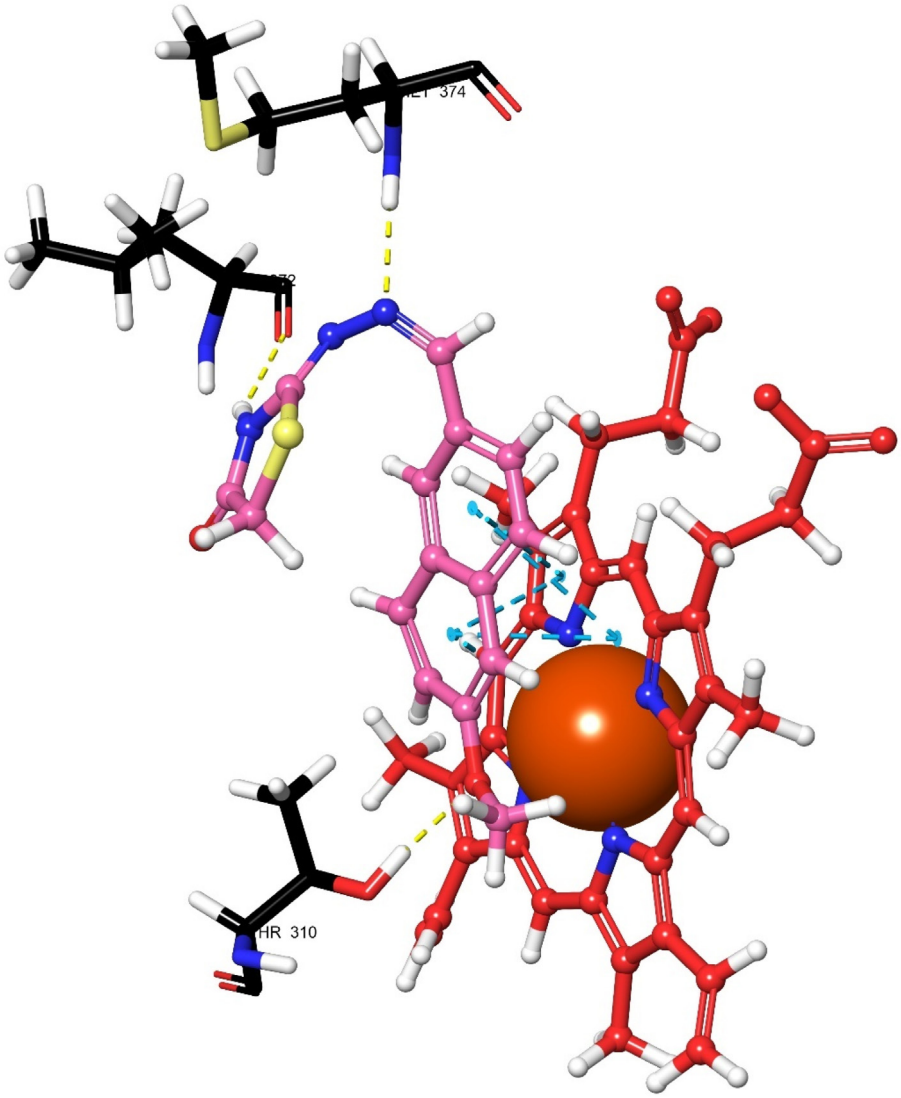

Fig. 8. The aspect of **2u**-Aromatase enzyme complex as 3D (PDBID: 3EQM).

factors, the 3D poses of the effects on compound **2q** shown in (Fig. 11) were generated using PLS factor 5. According to FB-QSAR results, from strength to weak properties, the MAO-B inhibition activity of 1,3-disubstitutedhydrazone derivatives is influenced by steric, HBA, hydrophobic, electrostatic, and HBD effects.

The results revealed that naphthalene ring could be configured on 4th and/or 5th positions with small groups (but not with potential HBA group). In addition, it could be changed with bioisosteric replacement (such as quinoline and coumarin) or substituted monocyclic ring systems (such as benzene, pyridine, azoles). Furthermore, the 1st and 2nd position of naphthalene should not contain any hydrophobic and hydrogen acceptor atom or group (such as halogens). On the other hand, both hydrophobic and H-bonds analyses showed that the thiazole hydrazone core is the main pharmacophore group, thus, it is necessary for the MAO inhibition. Despite that, the naphthalene substitution, as a steric group, could be made smaller, or at least less bulky to increase MAO-B activity. However, if this is done, the aromatase activity will be damaged because of the decreasing number of interactions with HEM protein as can be concluded from both *in-vitro* and *in-silico* studies.

All *in-silico* studies proved that the ethoxy acyl substitution is a significantly key moiety because of the interaction potential, and its interactions (with the FAD group and its peripheral residues). For further studies, our research group has been planning the replacement of the ethyl acetate group with HBA-rich groups like sulfonamide derivatives. As a result, this QSAR model could be used to determine new and current 1,3-disubstituted hydrazone derivatives that have MAO-B inhibition activity. Besides that, it could be a useful mediator model to develop new QSAR hypotheses of dual inhibitors of both monoamine oxidase enzyme and aromatase.

3. Materials and methods

3.1. Chemistry

All chemicals were purchased from Sigma-Aldrich Chemical Co (Sigma-Aldrich Corp., St. Louis, MO, USA) and Merck Chemicals (Merck KGaA, Darmstadt, Germany). All melting points (m.p.) were determined by MP90 digital melting point apparatus (Mettler Toledo, Ohio, USA) and were uncorrected. Reactions were monitored by thin-layer chromatography (TLC) using Silica Gel 60 F254

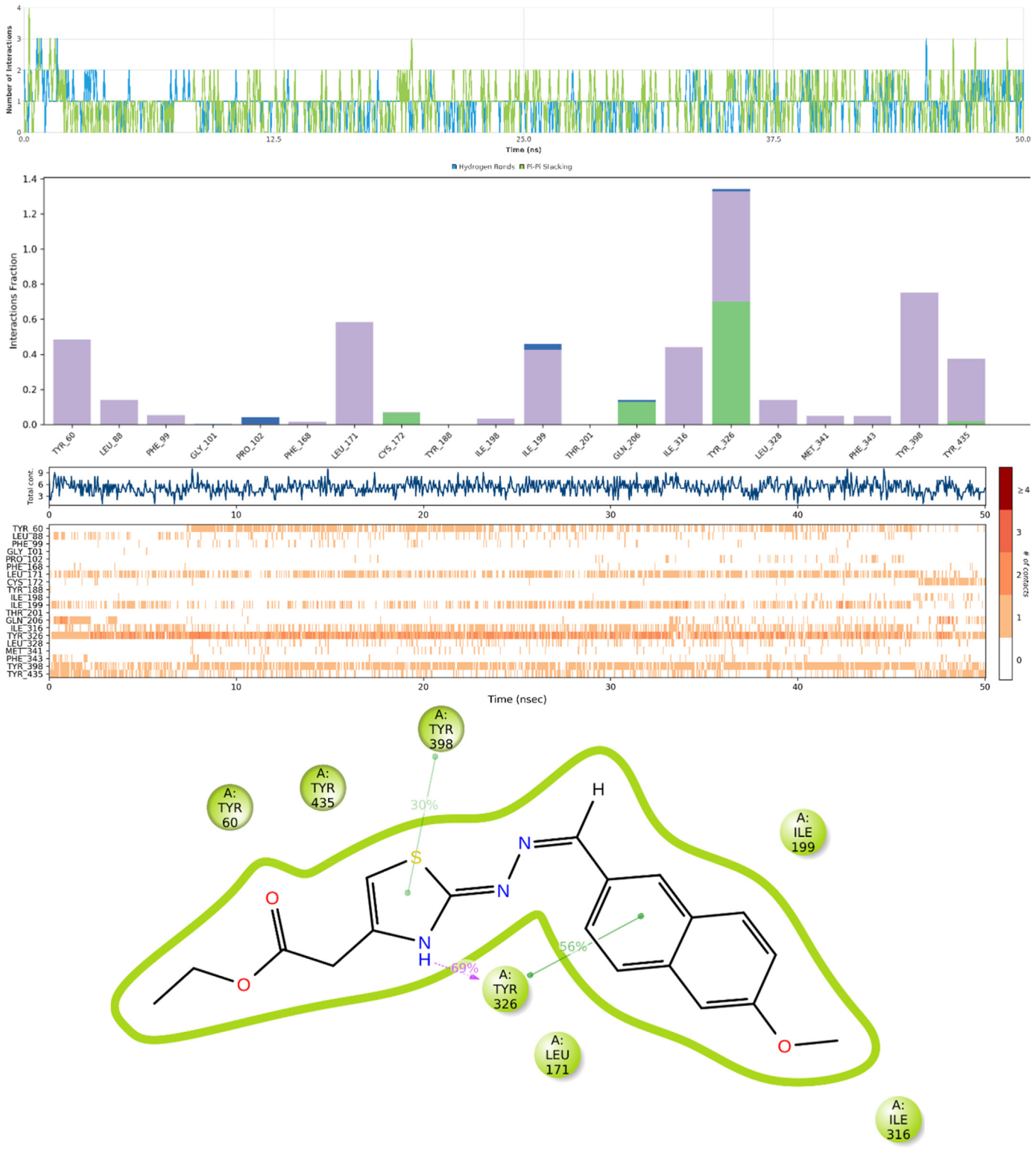

Fig. 9. The plots of Number of Interactions-time, the interactions fraction-residue, the residue-time, and the diagram of contact strength (cutoff = 30%) as 2D pose of **2q**-MAO-B complex, respectively.

TLC plates (Merck KGaA, Darmstadt, Germany). ^{1}H NMR and ^{13}C NMR spectral analyses were achieved using a Bruker digital FT-NMR spectrometer (Bruker Bioscience, Billerica, MA, USA) which was set to 300 MHz and 75 MHz respectively. Samples were prepared in DMSO-d_6 for those NMR analyses; Mass analysis was achieved using Shimadzu 8040 LC/MS/MS system (Shimadzu, Tokyo, Japan). Elemental analyses were performed on a Leco 932 CHNS analyzer (Leco, Michigan, USA).

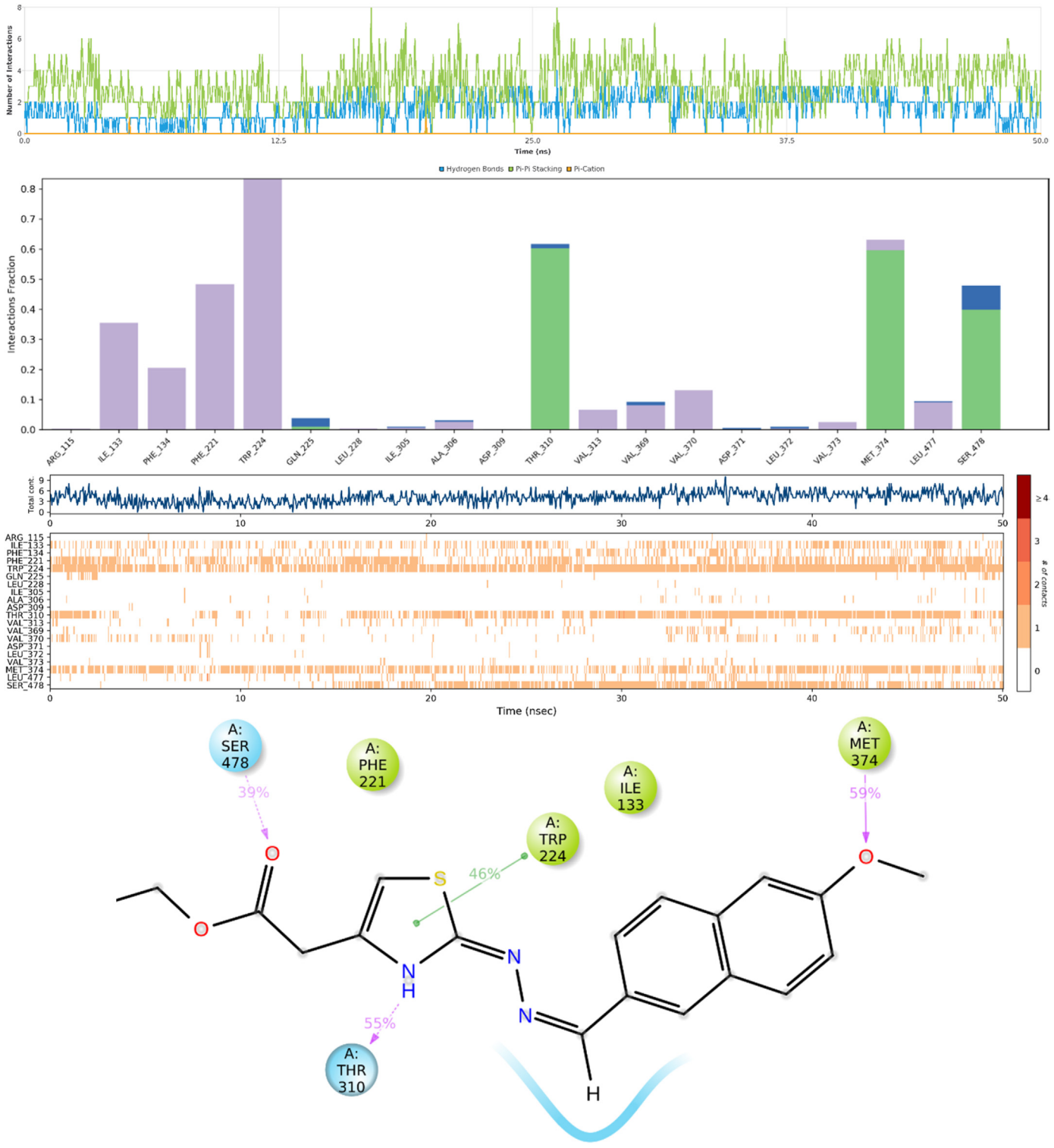

Fig. 10. The plots of the Number of Interactions-time, interactions fraction-residue, residue-time, and contact strength (cutoff = 30%) of 2q-MAO-B complex, respectively.

3.1.1. Synthesis of 2-((6-methoxynaphthalen-2-yl)methylene) hydrazin-1-carbothioamide (1)

6-methoxy-2-naphthaldeyde (1.565 g, 0.008 mol) was reacted with thiosemicarbazide (0.766 g, 0.008 mol) in ethanol under reflux. Reaction completion was controlled using TLC. The mixture was filtered while hot after the reaction was finished. Shiny colourless to white residue was obtained in pure form.

3.1.2. General synthesis of 2-(2-((6-methoxynaphthalen-2-yl) methylene)hydrazinyl)thiazole derivatives (2a-u)

Different substituents on positions 4 and/or 5 of thiazole ring were planned as illustrated in Scheme 1. Compound **1** was reacted with the corresponding reactants in 1:1 equivalent ratio to obtain their respective products as illustrated in Scheme 1. Reactants were refluxed in ethanol and the reaction ending was determined using

Table 3
The validation values of the FB-QSAR model.

#Factors	S.D.	R^2	Stability	F	P	RMSE	Q^2	Pearson-r
1	0.4824	0.6057	0.9613	58.4	$3.411e^{-09}$	0.65	−0.8015	−0.1132
2	0.3943	0.7434	0.8983	53.6	$1.181e^{-11}$	0.66	−0.8718	−0.1621
3	0.3489	0.8045	0.8197	49.4	$7.685e^{-13}$	0.63	−0.7114	−0.2581
4	0.2495	0.9028	0.4306	81.3	$3.222e^{-17}$	0.65	−0.7819	−0.3363
5*	0.2033	0.9373	0.2656	101.7	$1.894e^{-19}$	0.67	−0.9344	−0.3225

Table 4
FB-QSAR results: Gaussian (steric, Electrostatic, Hydrophobic, HBA and HBD) effects.

# Factors	Steric	Electrostatic	Hydrophobic	HBA	HBD
1	0.3366	0.1185	0.1238	0.1427	0.2783
2	0.3540	0.1438	0.1396	0.1598	0.2028
3	0.3162	0.1308	0.1718	0.1838	0.1974
4	0.2728	0.1416	0.2172	0.2238	0.1446
5*	0.2636	0.1531	0.2208	0.223	0.1403

TLC. After the reaction was finished, the mixture was filtered while hot to obtain the final product in pure form.

2-(2-((6-methoxynaphthalen-2-yl)methylene)hydrazinyl)-4-phenylthiazole, **2a**, m. p. 246–247 °C, ^{1}H NMR (300 MHz) (DMSO-d_6) δ (ppm): 3.89 (s, H, OMe), 7.20 (dd, J_1 = 2.52 Hz, J_2 = 8.88 Hz, H, Ar–H), 7.30–7.35 (m, 3H, Ar–H), 7.39–7.44 (m, 2H, Ar–H), 7.83–7.90 (m, 5H, Ar–H), 7.97 (s, H, Ar–H), 8.16 (s, H, H–C=N), 12.19 (brs, H, N–H). ^{13}C NMR (300 MHz) (DMSO-d_6) δ (ppm): 55.78 (OMe), 104.05, 106.84, 119.55, 123.12, 125.98, 127.90, 127.95, 128.74, 129.08, 130.24, 130.35, 135.19, 135.31, 142.06 (H–C=N), 151.08, 158.47, 168.68. For $C_{21}H_{17}N_3OS$ calculated: Elem. Anal.: C, 62.36%; H, 3.99%; N, 13.85%; O, 11.87%; S, 7.93%, found: C, 62.33%; H, 3.97%; N, 13.857%; O, 11.86%; S, 7.97%. HRMS (m/z): $[M + 1]^+$ calculated: 360.1165; found: 360.1156.

2-(2-((6-methoxynaphthalen-2-yl)methylene)hydrazinyl)-4-(*p*-tolyl)thiazole, **2b**, m. p. 243–244 °C, ^{1}H NMR (300 MHz) (DMSO-d_6) δ (ppm): 2.32 (s, 3H, Me), 3.89 (s, 3H, OMe), 7.18–7.25 (m, 4H, Ar–H), 7.35 (d, J = 2.46 Hz, H, Ar–H), 7.75 (d, J = 8.13 Hz, 2H, Ar–H), 7.83–7.89 (m, 3H, Ar–H), 7.96 (s, H, Ar–H), 8.16 (s, H, H–C=N), 12.16 (brs, H, N–H). ^{13}C NMR (300 MHz) (DMSO-d_6) δ (ppm): 21.27 (Me), 55.77 (OMe), 103.12, 106.84, 119.54, 123.12, 125.93, 127.90, 128.74, 129.64, 130.23, 130.36, 132.56, 135.30, 137.24, 141.97 (H–C=N), 158.46, 168.58. For $C_{22}H_{19}N_3OS$ calculated: Elem. Anal.: C, 70.75%; H, 5.13%; N, 11.25%; O, 4.28%; S, 8.59%, found: C, 70.72%; H, 5.12%; N, 11.26%; O, 4.30%; S, 8.61%. HRMS (m/z): $[M + 1]^+$ calculated: 374.1322; found: 374.1319.

2-(2-((6-methoxynaphthalen-2-yl)methylene)hydrazinyl)-4-(3-methoxyphenyl)thiazole, **2c**, m. p. 235–236 °C, ^{1}H NMR (300 MHz) (DMSO-d_6) δ (ppm): 3.80 (s, 3H, OMe), 3.89 (s, 3H, OMe), 7.18–7.22 (m, H, Ar–H), 7.35–7.36 (m, H, Ar–H), 7.37 (s, H, Ar–H), 7.41–7.43 (m, H, Ar–H), 7.46 (s, H, Ar–H), 7.86 (s, 3H, Ar–H), 7.90 (s, H, Ar–H), 7.97 (s, H, Ar–H), 7.99 (s, H, Ar–H), 8.16 (s, H, H–C=N), 12.32 (brs, H, N–H). ^{13}C NMR (300 MHz) (DMSO-d_6) δ (ppm): 55.50 (OMe), 55.79 (OMe), 106.85, 111.24, 113.68, 113.88, 114.46, 118.38, 119.56, 120.61, 123.12, 127.94, 128.69, 129.89, 130.13, 130.29, 135.33, 142.26 (H–C=N), 159.97. For $C_{22}H_{19}N_3O_2S$ calculated: Elem. Anal.: C, 67.84%; H, 4.92%; N, 10.79%; O, 8.22%; S, 8.23%, found: C, 67.79%; H, 4.87%; N, 10.82%; O, 8.26%; S, 8.26%. HRMS (m/z): $[M + 1]^+$ calculated: 390.1271; found: 390.1270.

2-(2-((6-methoxynaphthalen-2-yl)methylene)hydrazinyl)-4-(4-methoxyphenyl)thiazolel, **2d**, m. p. 239–240 °C, ^{1}H NMR (300 MHz) (DMSO-d_6) δ (ppm): 3.79 (s, 3H, Ph-OMe), 3.89 (s, 3H, Naph-OMe), 6.97 (d, J = 8.88 Hz, 2H, Ar–H), 7.16 (s, H, Ar–H), 7.19 (dd, J_1 = 2.52 Hz, J_2 = 8.94 Hz, H, Ar–H), 7.35 (d, J = 2.44 Hz, H, Ar–H), 7.80 (d, J = 8.79 Hz, 2H, Ar–H), 7.86–7.93 (m, 3H, Ar–H), 7.96 (s, H, Ar–H), 8.15 (s, H, H–C=N), 12.15 (brs, H, N–H). ^{13}C NMR (300 MHz) (DMSO-d_6) δ (ppm): 55.61 (OMe), 101.90, 106.84, 114.43, 119.54, 123.12, 127.30, 128.08, 128.74, 130.22, 130.38, 135.29, 141.93 (H–C=N), 158.46, 159.24, 168.55. For $C_{22}H_{19}N_3O_2S$ calculated: Elem. Anal.: C, 67.84%; H, 4.92%; N, 10.79%; O, 8.22%; S, 8.23%, found: C, 67.80%; H, 4.90%; N, 10.81%; O, 8.24%; S, 8.25%. HRMS (m/z): $[M + 1]^+$ calculated: 390.1271; found: 390.1271.

4-(3-chlorophenyl)-2-(2-((6-methoxynaphthalen-2-yl)methylene)hydrazinyl)thiazole, **2e**, m. p. 226–227 °C, ^{1}H NMR (300 MHz) (DMSO-d_6) δ (ppm): 3.89 (s, 3H, OMe), 7.20 (dd, J_1 = 2.53 Hz, J_2 = 8.91 Hz, H, Ar–H), 7.35–7.38 (m, 2H, Ar–H), 7.44 (d, J = 7.80 Hz, H, Ar–H), 7.51 (s, H, Ar–H), 7.82–7.85 (m, H, Ar–H), 7.87 (s, 2H, Ar–H), 7.90–7.92 (m, 2H, Ar–H), 7.98 (s, H, Ar–H), 8.17 (s, H, H–C=N), 12.22 (brs, H, N–H). ^{13}C NMR (300 MHz) (DMSO-d_6) δ (ppm): 55.79 (OMe), 105.68, 106.85, 119.56, 123.11, 124.51, 125.67, 127.70, 127.90, 128.06, 128.72, 130.24, 131.02, 133.93, 135.35, 137.15, 142.40 (H–C=N), 158.50, 168.80. For $C_{21}H_{16}ClN_3OS$ calculated: Elem. Anal.: C, 64.03%; H, 4.09%; Cl, 9.00%; N, 10.67%; O, 4.06%; S, 8.14%, found: C, 64.01%; H, 4.06%; Cl, 9.02%; N, 10.68%; O, 4.07%; S, 8.13%. HRMS (m/z): $[M + 1]^+$ calculated: 394.0775; found: 394.0792.

4-(4-chlorophenyl)-2-(2-((6-methoxynaphthalen-2-yl)methylene)hydrazinyl)thiazole, **2f**, m. p. 255–256 °C, ^{1}H NMR (300 MHz) (DMSO-d_6) δ (ppm): 3.89 (s, 3H, OMe), 7.20 (dd, J_1 = 2.53 Hz, J_2 = 8.91 Hz, H, Ar–H), 7.35 (d, H, Ar–H), 7.40 (s, H, Ar–H), 7.47 (d, J = 8.63 Hz, 2H, Ar–H), 7.89–7.89 (m, 5H, Ar–H), 7.97 (s, H, ArH), 8.17 (s, H, H–C=N), 12.20 (brs, H, N–H). ^{13}C NMR (300 MHz) (DMSO-d_6) δ (ppm): 55.77 (OMe), 104.86, 106.84, 199.55, 123.11, 127.66, 127.90, 128.73, 129.09, 130.24, 130.29, 132.38, 134.04, 135.34, 142.26 (H–C=N), 149.83, 158.49, 168.83. For $C_{21}H_{16}ClN_3OS$ calculated: Elem. Anal.: C, 64.03%; H, 4.09%; Cl, 9.00%; N, 10.67%; O, 4.06%; S, 8.14%, found: C, 64.00%; H, 4.08%; Cl, 9.02%; N, 10.69%; O, 4.07%; S, 8.13%. HRMS (m/z): $[M + 1]^+$ calculated: 394.0775; found: 394.0767.

4-(3-fluorophenyl)-2-(2-((6-methoxynaphthalen-2-yl)methylene)hydrazinyl)thiazole, **2g**, m. p. 235–236 °C, ^{1}H NMR (300 MHz) (DMSO-d_6) δ (ppm): 3.89 (s, 3H, OMe), 7.19 (dd, J_1 = 2.43 Hz, J_2 = 8.94 Hz, H, Ar–H), 7.35 (s, H, Ar–H), 7.47 (s, H, Ar–H), 7.62–7.66 (m, H, Ar–H), 7.70–7.77 (m, H, Ar–H), 7.86 (s, 3H, Ar–H), 7.89 (s, H, Ar–H), 7.97 (s, H, Ar–H), 7.99 (s, H, Ar–H), 8.18 (s, H, H–C=N), 12.34 (brs, H, N–H). ^{13}C NMR (300 MHz) (DMSO-d_6) δ (ppm): 55.77 (OMe), 105.59, 106.85, 112.37, 112.67, 114.81, 119.57, 122.03, 123.10, 124.33, 127.91, 128.37, 128.72, 130.25, 131.15, 135.36, 142.46, 143.46 (H–C=N), 158.50, 164.60, 168.77. For $C_{21}H_{16}FN_3OS$ calculated: Elem. Anal.: C, 66.83%; H, 4.27%; F, 5.03%; N, 11.13%; O, 4.24%; S, 8.50%, found: C, 66.79%; H, 4.26%; F, 5.02%; N, 11.16%; O, 4.26%; S, 8.51%. HRMS (m/z): $[M + 1]^+$ calculated: 378.1071; found: 378.1065.

4-(4-fluorophenyl)-2-(2-((6-methoxynaphthalen-2-yl)methylene)hydrazinyl)thiazole, **2h**, m. p. 240–241 °C, ^{1}H NMR (300 MHz) (DMSO-d_6) δ (ppm): 3.89 (s, 3H, OMe), 7.18–7.21 (m, H, Ar–H), 7.24–7.31 (m, 3H, Ar–H), 7.35 (s, H, Ar–H), 7.86–7.93 (m, 5H, Ar–H), 7.96 (s, H, Ar–H), 8.16 (s, H, H–C=N) 12.19 (brs, H, N–H). ^{13}C NMR (300 MHz) (DMSO-d_6) δ (ppm): 55.77 (OMe), 103.79, 106.84, 115.76, 116.05, 119.55, 123.11, 127.90, 128.00, 128.74, 131.82, 135.33, 142.19 (H–C=N), 149.98, 158.48, 160.45, 163.68, 168.79. For $C_{21}H_{16}FN_3OS$ calculated: Elem. Anal.: C, 66.83%; H, 4.27%; F, 5.03%;

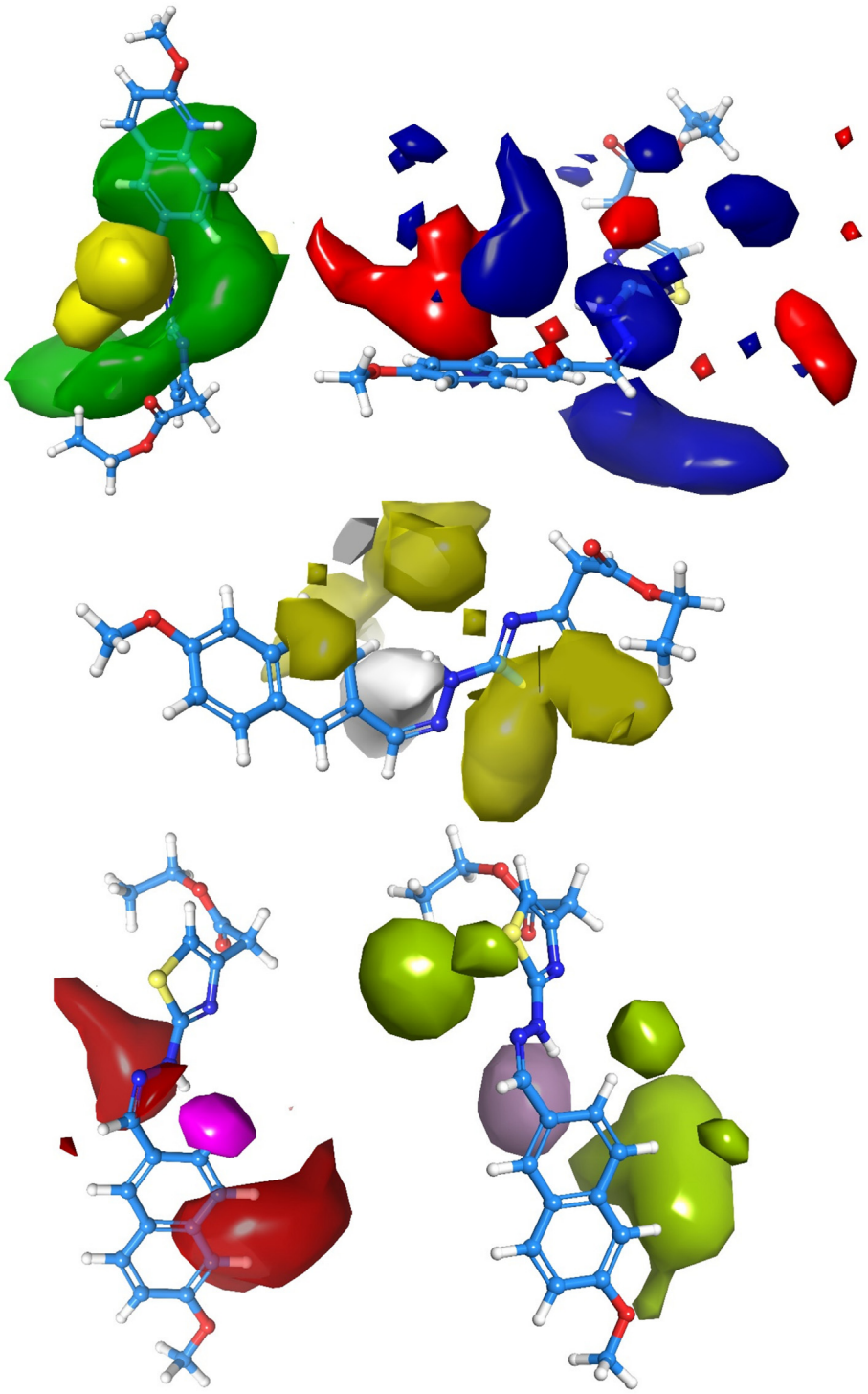

Fig. 11. 3D poses of the effects on **2q**: steric (positive effect (+): green, negative effect (−): yellow), electrostatic (+: blue, -: red), hydrophobic (+: yellow, -: white), HBA (+:red, -:magenta), and HBD (+:plum, -: yellow-green), respectively.

N, 11.13%; O, 4.24%; S, 8.50%, found: C, 66.79%; H, 4.25%; F, 5.00%; N, 11.09%; O, 4.22%; S, 8.49%. HRMS (*m*/*z*): $[M + 1]^+$ calculated: 378.1071; found: 378.1069.

4-(2-(2-((6-methoxynaphthalen-2-yl)methylene)hydrazinyl) thiazol-4-yl)benzonitrile, **2i**, m. p. 273–274 °C, ^{1}H NMR (300 MHz) (DMSO-d_6) δ (ppm): 3.89 (s, 3H, OMe), 7.20 (dd, $J_1 = 2.53$ Hz, $J_2 =$ 8.91 Hz, H, Ar–H), 7.35 (d, $J = 2.46$ Hz, H, Ar–H), 7.65 (s, H, Ar–H), 7.82–7.89 (m, 5H, Ar–H), 7.98 (s, H, Ar–H), 8.04 (d, $J = 8.55$ Hz, 2H, Ar–H), 8.18 (s, H, H–C=N), 12.26 (brs, H, N–H). ^{13}C NMR (300 MHz) (DMSO-d_6) δ (ppm): 55.78 (OMe), 106.84, 107.95, 119.47 (CN), 119.57, 123.10, 126.58, 127.91, 128.12, 128.72, 130.21, 130.26, 133.17, 135.37, 139.26, 142.55 (H–C=N), 149.34, 158.52, 169.02. For $C_{22}H_{16}N_4OS$ calculated: Elem. Anal.: C, 68.73%; H, 4.19%; N, 14.57%; O, 4.16%; S, 8.34%, found: C, 68.71%; H, 4.17%; N, 14.58%; O, 4.18%; S, 8.35%. HRMS (*m*/*z*): $[M + 1]^+$ calculated: 385.1118; found: 385.1131.

2-(2-((6-methoxynaphthalen-2-yl)methylene)hydrazinyl)-4-(3-nitrophenyl)thiazole, **2j**, m. p. 235–236 °C, ^{1}H NMR (300 MHz) (DMSO-d_6) δ (ppm): 3.89 (s, 3H, OMe), 7.20 (dd, $J_1 = 2.53$ Hz, $J_2 =$

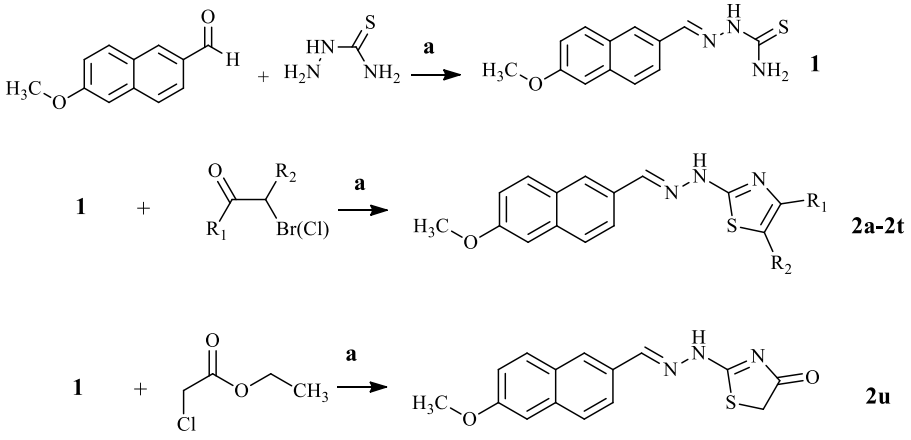

	R_1	R_2			
2a	phenyl	H	**2k**	4-nitrophenyl	H
2b	4-methylphenyl	H	**2l**	4-(methylsulfonyl)phenyl	H
2c	3-methoxyphenyl	H	**2m**	(1,1'-biphenyl)-4-yl	H
2d	4-methoxyphenyl	H	**2n**	naphthalen-2-yl	H
2e	3-chlorophenyl	H	**2o**	3,4-dichlorophenyl	H
2f	4-chlorophenyl	H	**2p**	benzofuran-2-yl	H
2g	3-fluorophenyl	H	**2q**	-CH_2COOEt	H
2h	4-fluorophenyl	H	**2r**	CH_3	CH_3
2i	4-cyanophenyl	H	**2s**	CH_3	-COOEt
2j	3-nitrophenyl	H	**2t**	phenyl	CH_3
2u	-	-			

Scheme 1. Synthesis plan. a: EtOH, Reflux.

8.91 Hz, H, Ar−H), 7.35 (d, J = 2.43 Hz, H, Ar−H), 7.67−7.74 (m, 2H, Ar−H), 7.87−7.90 (m, 3H, Ar−H), 7.99 (s, H, Ar−H), 8.14 (dd, $J1$ = 0.84 Hz, $J2$ = 2.37 Hz, H, Ar−H), 8.17 (s, H, H−C═N), 8.31 (m, H, Ar−H), 8.69 (t, J = 2.43 Hz, H, Ar−H), 12.32 (brs, H, N−H). ^{13}C NMR (300 MHz) (DMSO-d_6) δ (ppm): 55.78 (OMe), 106.84, 119.57, 120.41, 122.49, 123.10, 127.91, 128.12, 128.71, 130.19, 130.26, 130.71, 132.03, 135.38, 136.67, 142.54 (H−C═N), 148.64, 148.77, 158.52, 169.04. For $C_{21}H_{16}N_4O_3S$ calculated: Elem. Anal.: C, 62.36%; H, 3.99%; N, 13.85%; O, 11.87%; S, 7.93%, found: C, 62.32%; H, 3.97%; N, 13.86%; O, 11.89%; S, 7.96%. HRMS (m/z): $[M + 1]^+$ calculated: 405.1016; found: 405.1019.

2-(2-((6-methoxynaphthalen-2-yl)methylene)hydrazinyl)-4-(4-nitrophenyl)thiazole, **2k**, m. p. 270−272 °C, ^{1}H NMR (300 MHz) (DMSO-d_6) δ (ppm): 3.89 (s, 3H, OMe), 7.20 (dd, J_1 = 2.52 Hz, J_2 = 8.91 Hz, H, Ar−H), 7.35 (d, J = 2.4 Hz, H, Ar−H), 7.23 (s, H, Ar−H), 7.80−7.89 (m, 3H, Ar−H), 7.98 (s, H, Ar−H), 8.11 (d, J = 8.99 Hz, 2H, Ar−H), 8.18 (s, H, H−C═N), 8.28 (d, J = 9.02 Hz, 2H, Ar−H), 12.30 (brs, H, N−H). ^{13}CNMR (300 MHz) (DMSO-d_6) δ (ppm): 55.78 (OMe), 106.85, 108.97, 119.57, 123.10, 124.58, 126.79, 127.91, 128.14, 128.71, 130.18, 130.26, 135.39, 141.16, 142.64 (H−C═N), 146.66, 149.04, 158.53, 169.12. For $C_{21}H_{16}N_4O_3S$ calculated: Elem. Anal.: C, 62.36%; H, 3.99%; N, 13.85%; O, 11.87%; S, 7.93%, found: C, 62.35%; H, 3.95%; N, 13.87%; O, 11.89%; S, 7.94%. HRMS (m/z): $[M + 1]^+$ calculated: 405.1016; found: 405.1015.

2-(2-((6-methoxynaphthalen-2-yl)methylene)hydrazinyl)-4-(4-(methylsulfonyl)phenyl)thiazole, **2l**, m.p. 292−293 °C, ^{1}H NMR (300 MHz) (DMSO-d_6) δ (ppm): 3.24 (s, 3H, SO2Me), 3.89 (s, 3H, OMe), 7.20 (dd, J_1 = 2.51 Hz, J_2 = 8.91 Hz, H, Ar−H), 7.36 (d, J =

2.46 Hz, H, Ar−H), 7.65 (s, H, Ar−H), 7.87 (s, 2H, Ar−H), 7.90 (s, H, Ar−H), 7.95 (s, H, Ar−H), 7.97 (s, H, Ar−H), 7.98 (s, H, Ar−H), 8.12 (d, $J = 8.58$ Hz, 2H, Ar−H), 8.17 (s, H, H−C═N), 12.31 (brs, H, N−H). ^{13}C NMR (300 MHz) (DMSO-d_6) δ (ppm): 44.05 (SO2Me), 55.78 (OMe), 106.82, 107.66, 119.59, 123.09, 126.53, 127.92, 127.99, 128.13, 128.71, 130.20, 130.27, 135.37, 139.66, 142.48 (H−C═N), 149.39, 158.51, 169.01. For $C_{22}H_{19}N_3O_3S_2$ calculated: Elem. Anal.: C, 60.39%; H, 4.38%; N, 9.60%; O, 10.97%; S, 14.66%, found: C, 60.35%; H, 4.35%; N, 9.61%; O, 10.99%; S, 14.70%. HRMS (m/z): $[M + 1]^+$ calculated: 348.0941; found: 438.0947.

4-([1,1′-biphenyl]-4-yl)-2-(2-((6-methoxynaphthalen-2-yl) methylene)hydrazinyl)thiazole, **2m**, m.p. 240−241 °C, ^{1}H NMR (300 MHz) (DMSO-d_6) δ (ppm): 3.89 (s, 3H, OMe), 7.20 (dd, $J_1 =$ 2.54 Hz, $J_2 = 8.88$ Hz, H, Ar−H), 7.35−7.41 (m, 3H, Ar−H), 7.45−7.50 (m, 2H, Ar−H), 7.71−7.74 (m, 4H, Ar−H), 7.86−7.90 (m, 3H, Ar−H), 7.95 (s, H, Ar−H), 7.98 (s, H, Ar−H), 8.17 (s, H, H−C═N), 12.24 (brs, H, N−H). ^{13}C NMR (300 MHz) (DMSO-d_6) δ (ppm): 55.78 (OMe), 104.30, 106.82, 119.67, 123.10, 126.55, 126.94, 127.31, 127.91, 128.74, 130.25, 130.33, 134.29, 135.32, 139.49, 140.11, 142.13 (H−C═N), 158.47, 168.72. For $C_{27}H_{21}N_3OS$ calculated: Elem. Anal.: C, 74.46%; H, 4.86%; N, 9.65%; O, 3.67%; S, 7.36%, found: C, 74.44%; H, 4.82%; N, 9.66%; O, 3.69%; S, 7.38%. HRMS (m/z): $[M + 1]^+$ calculated: 436.1478; found: 436.1485.

2-(2-((6-methoxynaphthalen-2-yl)methylene)hydrazinyl)-4-(naphthalen-2-yl)thiazole, **2n**, m. p. 254−256 °C, ^{1}H NMR (300 MHz) (DMSO-d_6) δ (ppm): 3.89 (s, 3H, OMe), 7.20 (dd, $J_1 =$ 2.46 Hz, $J_2 = 8.88$ Hz, H, Ar−H), 7.36 (s, H, Ar−H), 7.50 (s, H, Ar−H), 7.52−7.58 (m, 2H, Ar−H), 7.87 (s, H, Ar−H), 7.88−7.90 (m, H, Ar−H), 7.93−8.01 (m, 5H, Ar−H), 8.19 (d, $J = 5.83$ Hz, H, Ar−H), 8.40 (d, $J =$ 7.45 Hz, H, Ar−H), ^{13}C NMR (300 MHz) (DMSO-d_6) δ (ppm): 55.80 (OMe), 104.92, 106.86, 119.56, 123.13, 124.58, 126.02, 126.91, 128.05, 128.23, 128.73, 129.97, 130.27, 131.58, 132.43, 132.91, 133.40, 133.62, 135.36, 142.43, 143.31, 150.64, 158.50, 167.52, 168.77. For $C_{25}H_{19}N_3OS$ calculated: Elem. Anal.: C, 73.32%; H, 4.68%; N, 10.26%; O, 3.91%; S, 7.83%, found: C, 73.29%; H, 4.66%; N, 10.28%; O, 3.93%; S, 7.85%. HRMS (m/z): $[M + 1]^+$ calculated: 410.1322; found: 410.1320.

4-(3,4-dichlorophenyl)-2-(2-((6-methoxynaphthalen-2-yl) methylene)hydrazinyl)thiazole, **2o**, m. p. 254−256 °C, ^{1}H NMR (300 MHz) (DMSO-d_6) δ (ppm): 3.89 (s, 3H, OMe), 7.20 (dd, $J_1 =$ 2.53 Hz, $J_2 = 8.91$ Hz, H, Ar−H), 7.35 (d, $J = 2.43$ Hz, H, Ar−H), 7.57 (s, H, Ar−H), 7.67 (d, $J = 8.45$ Hz, H, Ar−H), 7.86−7.90 (m, 4H, Ar−H), 7.98 (s, H, Ar−H), 8.10 (d, $J = 2.05$ Hz, H, Ar−H), 8.17 (s, H, H−C═N), 12.23 (brs, H, N−H). ^{13}C NMR (300 MHz) (DMSO-d_6) δ (ppm): 55.79 (OMe), 106.33, 106.85, 119.56, 123.10, 126.03, 127.63, 127.91, 128.10, 128.72, 130.14, 130.20, 13026, 131.34, 131.88, 135.37, 135.70, 142.53 (H−C═N), 148.41, 158.51, 168.92. For $C_{21}H_{15}Cl_2N_3OS$ calculated: Elem. Anal.: C, 58.89%; H, 3.53%; Cl, 16.55%; N, 9.81%; O, 3.74%; S, 7.49%, found: C, 58.86%; H, 3.51%; Cl, 16.56%; N, 9.83%; O, 3.75%; S, 7.50%. HRMS (m/z): $[M + 1]^+$ calculated: 428.0386; found: 428.0385.

4-(benzofuran-2-yl)-2-(2-((6-methoxynaphthalen-2-yl)methylene)hydrazinyl)thiazole, **2p**, m. p. 227−228 °C, ^{1}H NMR (300 MHz) (DMSO-d_6) δ (ppm): 3.89 (s, 3H, OMe), 7.20 (dd, $J_1 = 2.46$ Hz, $J_2 =$ 8.88 Hz, H, Ar−H), 7.24−7.30 (m, 2H, Ar−H), 7.33−7.36 (m, 3H, Ar−H), 7.59−7.62 (m, H, Ar−H), 7.66−7.69 (m, H, Ar−H), 7.87−7.90 (m, 3H, Ar−H), 7.99 (s, H, Ar−H), 8.17 (s, H, H−C═N), 12.35 (brs, H, N−H). ^{13}C NMR (300 MHz) (DMSO-d_6) δ (ppm): 55.78 (OMe), 102.76, 106.57, 106.83, 111.46, 119.59, 121.84, 123.10, 123.74, 125.11, 127.93, 128.18, 128.71, 128.94, 130.16, 130.28, 135.39, 142.41, 142.66 (H−C═N), 152.48, 154.56, 158.53, 169.36. For $C_{23}H_{17}N_3O_2S$ calculated: Elem. Anal.: C, 69.15%; H, 4.29%; N, 10.52%; O, 8.01%; S, 8.03%, found: C, 69.12%; H, 4.26%; N, 10.54%; O, 8.03%; S, 8.05%. HRMS (m/z): $[M + 1]^+$ calculated: 400.1114; found: 400.1115.

Ethyl 2-(2-(2-((6-methoxynaphthalen-2-yl)methylene)hydrazinyl)thiazol-4-yl)acetate, **2q**, m. p 147−148 °C, ^{1}H NMR (300 MHz) (DMSO-d_6) δ (ppm): 1.21 (t, $J = 14.19$ Hz, 3H, Aliph-Me), 3.74 (s, 2H, CH_2COO), 3.89 (s, 3H, OMe), 4.12 (q, $J_1 = 7.09$ Hz, $J_2 = 14.16$ Hz, 2H, $COOCH_2$), 6.83 (s, H, Ar−H), 7.20 (dd, $J1 = 2.48$ Hz, $J2 = 8.91$ Hz, H, Ar−H), 7.36 (d, $J = 2.47$ Hz, H, Ar−H), 7.83−7.88 (m, 2H, Ar−H), 7.91−7.97 (m, 2H, Ar−H), 8.04 (s, H, Ar−H), 8.37 (s, H, H−C═N). ^{13}C NMR (300 MHz) (DMSO-d_6) δ (ppm): 14.55 (Me), 35.49 (CH_2COO), 55.81 (OMe), 61.06 ($COOCH_2$), 106.86, 107.01, 119.67, 123.26, 127.94, 128.59, 129.18, 129.55, 130.43, 135.75, 158.78, 169.81. NOTE: there might be a lost peak. For $C_{19}H_{19}N_3O_3S$ calculated: Elem. Anal.: C, 61.77%; H, 5.18%; N, 11.37%; O, 12.99%; S, 8.68%, found: C, 61.72%; H, 5.16%; N, 11.41%; O, 12.98%; S, 8.72%. HRMS (m/z): $[M + 1]^+$ calculated: 370.1220; found: 370.1232.

2-(2-((6-methoxynaphthalen-2-yl)methylene)hydrazinyl)-4,5-dimethylthiazole, **2r**, m.p. 217−218 °C, ^{1}H NMR (300 MHz) (DMSO-d_6) δ (ppm): 2.18 (s, 3H, thiazole-CH3), 2.22 (s, 3H, thiazole-CH_3), 3.90 (s, 3H, OMe), 7.22 (dd, $J_1 = 2.52$ Hz, $J_2 = 8.94$ Hz, H, Ar−H), 7.38 (d, $J = 2.43$ Hz, H, Ar−H), 7.87−7.98 (m, 3H, Ar−H), 8.09 (s, H, H−C═N), 8.39 (s, H, Ar−H). ^{13}C NMR (300 MHz) (DMSO-d_6) δ (ppm): 11.06 (thiazole-CH_3), 55.79 (OMe), 106.90, 119.73, 123.40, 127.92, 128.55, 129.38, 130.47, 135.90, 158.89. For $C_{17}H_{17}N_3OS$ Elem. Analysis calculated: C, 65.57%; H, 5.50%; N, 13.49%; O, 5.14%; S, 10.30%; found: C, 65.55%; H, 5.52%; N, 13.49%; O, 5.13%; S, 10.31%. HRMS (m/z): $[M + 1]^+$ calculated: 312.1165; found: 312.1150.

Ethyl 2-(2-((6-methoxynaphthalen-2-yl)methylene)hydrazinyl)-4-methylthiazole-5-carboxylate, **2s**, m.p. 252−253 °C, ^{1}H NMR (300 MHz) (DMSO-d_6) δ (ppm): 1.27 (t, $J = 7.10$ Hz, 3H, Aliph-Me), 2.48 (s, 3H, Ar-Me), 3.89 (s, 3H, OMe), 4.21 (q, $J_1 = 7.09$ Hz, $J_2 =$ 7.10, 2H, COOCH2), 7.19 (dd, $J_1 = 2.53$ Hz, $J_2 = 8.94$ Hz, H, Ar−H), 7.36 (d, $J = 2.47$ Hz, H, Ar−H), 7.83−7.90 (m, 3H, Ar−H), 8.01 (s, H, H−C═N), 8.26 (s, H, Ar−H), 9.88 (brs, H, N−H). ^{13}C NMR (300 MHz) (DMSO-d_6) δ (ppm): 14.79 (Aliph-Me), 17.39 (Ar-Me), 55.79 (OMe), 60.66 ($COOCH_2$), 106.84, 109.36, 119.62, 123.27, 127.95, 128.63, 128.82, 129.79, 130.40, 135.67, 145.70 (H−C═N), 158.12, 158.69, 162.30, 169.38, 180.94 (−COO−). For $C_{19}H_{19}N_3O_3S$ calculated: Elem. Anal.: C, 61.77%; H, 5.18%; N, 11.37%; O, 12.99%; S, 8.68%, found: C, 61.72%; H, 5.15%; N, 11.40%; O, 12.97%; S, 8.75%. HRMS (m/z): $[M + 1]^+$ calculated: 370.1220; found: 370.1216.

2-(2-((6-methoxynaphthalen-2-yl)methylene)hydrazinyl)-5-methyl-4-phenylthiazole, **2t**, m. p. 227−228 °C, ^{1}H NMR (300 MHz) (DMSO-d_6) δ (ppm): 2.42 (s, 3H, Me), 3.89 (s, 3H, OMe), 7.20 (dd, $J_1 =$ 2.52 Hz, $J_2 = 8.91$ Hz, H, Ar−H), 7.35−7.38 (m, 2H, Ar−H), 7.34−7.48 (m, 2H, Ar−H), 7.61−7.64 (m, 2H, Ar−H), 7.86−7.89 (m, 3H, Ar−H), 7.97 (s, H, Ar−H), 8.18 (s, H, H−C═N), 11.96 (brs, H, N−H). ^{13}C NMR (300 MHz) (DMSO-d_6) δ (ppm): 12.65 (Me), 55.78 (OMe), 106.84, 117.28, 119.57, 123.19, 127.88, 128.14, 128.53, 128.70, 128.84, 130.21, 130.26, 134.59, 135.39, 142.99 (H−C═N), 158.51, 164.98. For $C_{22}H_{19}N_3OS$ calculated: Elem. Anal.: C, 70.75%; H, 5.13%; N, 11.25%; O, 4.28%; S, 8.59%, found: C, 70.71%; H, 5.12%; N, 11.26%; O, 4.29%; S, 8.62%. HRMS (m/z): $[M + 1]^+$ calculated: 374.1322; found: 374.1316.

2-(2-((6-methoxynaphthalen-2-yl)methylene)hydrazinyl)thiazol-4(5H)-one, **2u**, m. p. 249−250 °C, ^{1}H NMR (300 MHz) (DMSO-d_6) δ (ppm): 3.89 (s, 3H, OMe), 3.92 (s, 2H, thiazol-4(5H)-one), 7.19 (dd, $J_1 = 2.52$ Hz, $J_2 = 8.88$ Hz, H, Ar−H), 7.85−7.94 (m, 3H, Ar−H), 8.11 (s, H, H−C═N), 8.51 (s, H, Ar−H), 11.99 (brs, H, N−H). ^{13}C NMR (300 MHz) (DMSO-d_6) δ (ppm): 33.50 (thiazol-4(5H)-one, 55.82 (OMe), 106.85, 119.69, 123.90, 127.87, 128.52, 130.13, 130.53, 136.10, 156.88, 158.89, 174.65 (carbonyl of thiazol-4(5H)-one). For $C_{17}H_{17}N_3O_2S$ calculated: Elem. Anal.: C, 62.36%; H, 5.23%; N, 12.83%; O, 9.77%; S, 9.79%, found: C, 62.34%; H, 5.24%; N, 12.82%; O, 9.79%; S, 9.79%. HRMS (m/z): $[M + 1]^+$ calculated: 300.0801; found: 300.0790.

3.2. Prediction of physicochemical and pharmacokinetic properties

Determination of drug-like properties, in other words, medicinal chemical profile, is important to evaluate the designed

compounds. The pharmacokinetic profile is also predicted via *in silico* methods as a preliminary evaluation in this stage. The active compounds might be considered in the future for *in vivo* pharmacokinetic studies as the current study is involved basically in the evaluation of the activity. Therefore, the medicinal chemistry and pharmacokinetic profiles of the designed compounds were calculated by Swiss-ADME web-based program [43].

3.3. In-vitro enzyme studies

3.3.1. MAO inhibitions

In-vitro MAO-A and MAO-B enzyme inhibition tests were performed as in previous studies [16,44]. The compounds were dissolved in dimethyl sulfoxide (DMSO) and added to the assay in at least 7 concentrations ranging from 10^{-3}-10^{-9} M. Moclobemide and selegiline were used as the positive inhibition controls in MAO-A and MAO-B inhibition tests, respectively.

3.3.2. Aromatase inhibition

In-vitro aromatase inhibition tests were performed using a kit procedure (Bio Vision, Aromatase (CYP19A) Inhibitor Screening Kit (Fluorometric)), as previously [34,45,46]. The compounds were dissolved in dimethyl sulfoxide (DMSO) and added to the assay in at least 7 concentrations ranging from 10^{-3}-10^{-9} M. Letrozole was used as a positive inhibition control.

3.4. In-silico studies

3.4.1. Molecular docking studies

Molecular docking studies were performed using an *in-silico* procedure to define the binding modes of active compound in the active regions of enzymes X-ray crystal structures of the monoamine oxidase (A and B) and aromatase enzymes (PDB ID: 2Z5X, 2V5Z, and 3EQM, respectively), were retrieved from the Protein Data Bank server (www.pdb.org, accessed April 01, 2021). Schrödinger Maestro [47] interface was used for the molecular docking study and the enzymes crystals were processed using the Protein Preparation Wizard protocol of the Schrödinger Suite 2020. Compounds were prepared using the LigPrep module [48] to correctly assign the protonation states as well as the atom types. Bond orders were assigned, and hydrogen atoms were added to the structures. The grid generation was formed using the Glide module [49], and docking runs were performed in standard precision docking mode (SP).

3.4.2. Molecular dynamic simulation (MDS) studies

Molecular dynamic (MD) simulations have been considered an important computational tool for evaluating the time-dependent stability the ligand-receptor complex. In this study, MDS for 50 ns were carried out to ensure the stability of the identified hits from the docking results. We performed Desmond application [41] using the standard force field (OPLS3e) of Schrodinger Suite with a transferable intermolecular potential with 3 points (TIP3P) water model followed by energy minimization of the complex. The neutralization of the system was achieved using Na+ and Cl− ions and 150 mM NaCl was added into dynamic condition. The molecular dynamic simulation was performed following the completion of the system setup. The radius of gyration (Rg), root mean square fluctuation (RMSF), and root mean square deviation (RMSD) values were calculated by Desmond application.

3.4.3. Building field-based QSAR (FB-QSAR) model and checking its validation

Clarifying the structure-activity relationship is one of the ultimate goals in pharmaceutical chemistry studies. Thus, it was aimed to contribute to the structure-activity relationship (SAR) by evaluating the data obtained from MAO-B inhibitors with a similar core structure in the literature. To build the QSAR model, the compounds that have hydrazone moiety were filtered, by summing up all MAO-B inhibitors with IC_{50} value ($logIC_{50} \geq 5.00$) from the ChEMBL database by our group (Accessed date: August 10, 2021; https://www.ebi.ac.uk/chembl/). About 61 compounds from 9521 compounds were obtained and minimized with the ConfGen application [50]. The pIC_{50} ($logIC_{50}$) values of them presented in Table S2 and then opened in 3D Field-Based QSAR interface for the QSAR study. The training set was set to 66% and the selection was made randomly. After the PLS factor was marked as 5, the QSAR model was built with standard settings. R^2, Q^2, pearson-r, stability, RMSE, F and P values were analyzed for the stability and validation of the obtained FB-QSAR model. The validation criterion thresholds for the previously described parameters [51] are as follows: $R^2 > 0.7$, $Q^2 > 0.7$, where the difference between R^2 and Q^2 is less than 0.1. Also, the Pearson correlation coefficients (Pearson-r), $|r_c|$, are equal to or greater than 0.3.

4. Conclusions

2-(2-((6-Methoxynaphthalen-2-yl)methylene)hydrazinyl)thiazole derivatives (**2a-2u**) were synthesized in this work. Monoamine oxidase A and B enzyme inhibitions of the obtained twenty-one compounds were tested at 10^{-3} and 10^{-4} M concentrations. Compounds **2j** and **2t** showed excellent inhibitory activity on the MAO-A enzyme, with a potency approximately 100 times higher than moclobemide. Compounds **2j**, **2k** and **2q** inhibited MAO-B, with very close or half the potency of selegiline. The inhibitory effects of compounds **2q** and **2u** on the aromatase enzyme were also found to be well-nigh to letrozole although not as much as standard drug. According to molecular docking studies, **2j** and **2t** fit into MAO-A enzyme while **2j**, **2k**, and **2q** were successfully docked to active site of MAO-B enzyme. The interaction with Gln206 was observed for compounds **2k** and **2q**, which is an important residue for the MAO-B selectivity that supports *in-vitro* results. Compounds **2q** and **2u** were determined to interact to HEM protein with π-π bonds which is a necessary for aromatase inhibition. Molecular dynamic studies were performed for **2q**-MAO-B and **2q**-aromatase complexes and ligand-enzyme stability was found to support molecular docking and *in-vitro* activity results. To clarify the structure-activity relationship, a Field-Based QSAR study was performed. As a result of its inhibitory activity against both MAO-B and aromatase, compound **2q** is a good example of an agent that can be used in special cases of breast cancer patients who suffer from neurodegenerative symptoms.

Author contributions

Conceptualization, L.Y., A.E.E., S.D. and D.N.; methodology, B.N.S., A.E.E., S.D. and D.N.; software, A.E.E., S.D. and D.N.; validation L.Y., A.E.E., S.D. and D.N.; formal analysis, A.E.E., S.D. and D.N.; investigation, A.E.E., S.D. and D.N.; resources, L.Y., A.E.E., S.D. and D.N.; data curation, L.Y., A.E.E., S.D. and D.N.; writing—original draft preparation, L.Y., A.E.E. and S.D. writing—review and editing, D.N. and B.N.S.; visualization, A.E.E., S.D. and D.N.; supervision, L.Y.; project administration, L.Y.; funding acquisition, L.Y. All authors have read and agreed to the published version of the manuscript.

Funding

This research was funded by Anadolu University Scientific Research Projects with grant number 2008S092" and "The APC was funded by Anadolu University".

Institutional review board statement

Not applicable.

Informed consent statement

Not applicable.

Data availability statement

Not applicable.

Sample availability

Samples of the compounds **2a-2u** are available from the authors.

Declaration of competing interest

The authors declare that they have no known competing financial interests or personal relationships that could have appeared to influence the work reported in this paper.

Acknowledgments

The authors presents their thanks to DOPNA laboratory, Anadolu University and Scientific Research Projects, Anadolu University.

Appendix A. Supplementary data

Supplementary data to this article can be found online at https://doi.org/10.1016/j.ejmech.2021.114097.

References

[1] N.T. Patel, R.R. Fritz, C.W. Abell, Isolation of pure, catalytically active human liver monoamine oxidase B: antibody complex, Biochem. Biophys. Res. Commun. 125 (1984) 748–754, https://doi.org/10.1016/0006-291x(84)90602-8.
[2] J.P. Johnston, Some observations upon a new inhibitor of monoamine oxidase in brain tissue, Biochem. Pharmacol. 17 (1968) 1285–1297, https://doi.org/10.1016/0006-2952(68)90066-x.
[3] J.P. Finberg, J.M. Rabey, Inhibitors of MAO-A and MAO-B in psychiatry and neurology, Front. Pharmacol. 7 (2016) 340, https://doi.org/10.3389/fphar.2016.00340.
[4] A.W.K. Yeung, M.G. Georgieva, A.G. Atanasov, N.T. Tzvetkov, Monoamine oxidases (MAOs) as privileged molecular targets in neuroscience: research literature analysis, Front. Mol. Neurosci. 12 (2019) 143, https://doi.org/10.3389/fnmol.2019.00143.
[5] A.Y. Deutch, R.H. Roth, Pharmacology and Biochemistry of Synaptic Transmission: Classic Transmitters, 2004, pp. 245–278, https://doi.org/10.1016/b978-012148660-0/50010-x.
[6] N.A. Murugan, C. Muvva, C. Jeyarajpandian, J. Jeyakanthan, V. Subramanian, Performance of force-field- and machine learning-based scoring functions in ranking MAO-B protein-inhibitor complexes in relevance to developing Parkinson's therapeutics, Int. J. Mol. Sci. 21 (2020), https://doi.org/10.3390/ijms21207648.
[7] F. Chimenti, E. Maccioni, D. Secci, A. Bolasco, P. Chimenti, A. Granese, O. Befani, P. Turini, S. Alcaro, F. Ortuso, M.C. Cardia, S. Distinto, Selective inhibitory activity against MAO and molecular modeling studies of 2-thiazolylhydrazone derivatives, J. Med. Chem. 50 (2007) 707–712, https://doi.org/10.1021/jm060869d.
[8] F. Chimenti, S. Carradori, D. Secci, A. Bolasco, P. Chimenti, A. Granese, B. Bizzarri, Synthesis and biological evaluation of novel conjugated coumarin-thiazole systems, J. Heterocycl. Chem. 46 (2009) 575–578, https://doi.org/10.1002/jhet.110.
[9] F. Chimenti, A. Bolasco, D. Secci, P. Chimenti, A. Granese, S. Carradori, M. Yanez, F. Orallo, F. Ortuso, S. Alcaro, Investigations on the 2-thiazolylhydrazyne scaffold: synthesis and molecular modeling of selective human monoamine oxidase inhibitors, Bioorg. Med. Chem. 18 (2010) 5715–5723, https://doi.org/10.1016/j.bmc.2010.06.007.
[10] F. Chimenti, D. Secci, A. Bolasco, P. Chimenti, A. Granese, S. Carradori, E. Maccioni, M.C. Cardia, M. Yanez, F. Orallo, S. Alcaro, F. Ortuso, R. Cirilli, R. Ferretti, S. Distinto, J. Kirchmair, T. Langer, Synthesis, semipreparative HPLC separation, biological evaluation, and 3D-QSAR of hydrazothiazole derivatives as human monoamine oxidase B inhibitors, Bioorg. Med. Chem. 18 (2010) 5063–5070, https://doi.org/10.1016/j.bmc.2010.05.070.
[11] D. Secci, A. Bolasco, S. Carradori, M. D'Ascenzio, R. Nescatelli, M. Yanez, Recent advances in the development of selective human MAO-B inhibitors: (hetero) arylidene-(4-substituted-thiazol-2-yl)hydrazines, Eur. J. Med. Chem. 58 (2012) 405–417, https://doi.org/10.1016/j.ejmech.2012.10.032.
[12] G. Raciti, P. Mazzone, A. Raudino, G. Mazzone, A. Cambria, Inhibition of rat liver mitochondrial monoamine oxidase by hydrazine-thiazole derivatives: structure-activity relationships, Bioorg. Med. Chem. 3 (1995) 1485–1491, https://doi.org/10.1016/0968-0896(95)00137-6.
[13] D. Secci, S. Carradori, A. Petzer, P. Guglielmi, M. D'Ascenzio, P. Chimenti, D. Bagetta, S. Alcaro, G. Zengin, J.P. Petzer, F. Ortuso, 4-(3-Nitrophenyl)thiazol-2-ylhydrazone derivatives as antioxidants and selective hMAO-B inhibitors: synthesis, biological activity and computational analysis, J. Enzym. Inhib. Med. Chem. 34 (2019) 597–612, https://doi.org/10.1080/14756366.2019.1571272.
[14] S. Distinto, M. Yanez, S. Alcaro, M.C. Cardia, M. Gaspari, M.L. Sanna, R. Meleddu, F. Ortuso, J. Kirchmair, P. Markt, A. Bolasco, G. Wolber, D. Secci, E. Maccioni, Synthesis and biological assessment of novel 2-thiazolylhydrazones and computational analysis of their recognition by monoamine oxidase B, Eur. J. Med. Chem. 48 (2012) 284–295, https://doi.org/10.1016/j.ejmech.2011.12.027.
[15] M. D'Ascenzio, S. Carradori, D. Secci, L. Mannina, A.P. Sobolev, C. De Monte, R. Cirilli, M. Yanez, S. Alcaro, F. Ortuso, Identification of the stereochemical requirements in the 4-aryl-2-cycloalkylidenhydrazinylthiazole scaffold for the design of selective human monoamine oxidase B inhibitors, Bioorg. Med. Chem. 22 (2014) 2887–2895, https://doi.org/10.1016/j.bmc.2014.03.042.
[16] I.O. Ates, A.E. Evren, B.N. Saglik, L. Yurttas, New indane derivatives containing 2-hydrazinothiazole as potential acetylcholinesterase and monoamine oxidase-B inhibitors, Z. Naturforsch. C J. Biosci. 76 (2021) 417–424, https://doi.org/10.1515/znc-2021-0058.
[17] N.O. Can, D. Osmaniye, S. Levent, B.N. Saglik, B. Korkut, O. Atli, Y. Ozkay, Z.A. Kaplancikli, Design, synthesis and biological assessment of new thiazolylhydrazine derivatives as selective and reversible hMAO-A inhibitors, Eur. J. Med. Chem. 144 (2018) 68–81, https://doi.org/10.1016/j.ejmech.2017.12.013.
[18] W.R. Miller, A.A. Larionov, Understanding the mechanisms of aromatase inhibitor resistance, Breast Cancer Res. 14 (2012) 201, https://doi.org/10.1186/bcr2931.
[19] C.J. Fabian, The what, why and how of aromatase inhibitors: hormonal agents for treatment and prevention of breast cancer, Int. J. Clin. Pract. 61 (2007) 2051–2063, https://doi.org/10.1111/j.1742-1241.2007.01587.x.
[20] A.S. Mayhoub, L. Marler, T.P. Kondratyuk, E.J. Park, J.M. Pezzuto, M. Cushman, Optimization of the aromatase inhibitory activities of pyridylthiazole analogues of resveratrol, Bioorg. Med. Chem. 20 (2012) 2427–2434, https://doi.org/10.1016/j.bmc.2012.01.047.
[21] R.W. Brueggemeier, J.C. Hackett, E.S. Diaz-Cruz, Aromatase inhibitors in the treatment of breast cancer, Endocr. Rev. 26 (2005) 331–345, https://doi.org/10.1210/er.2004-0015.
[22] R.W. Brueggemeier, Overview of the pharmacology of the aromatase inactivator exemestane, Breast Cancer Res. Treat. 74 (2002) 177–185, https://doi.org/10.1023/a:1016121822916.
[23] G. Wang, Z. Peng, Y. Li, Synthesis, anticancer activity and molecular modeling studies of novel chalcone derivatives containing indole and naphthalene moieties as Tubulin polymerization inhibitors, Chem. Pharm. Bull. (Tokyo) 67 (2019) 725–728, https://doi.org/10.1248/cpb.c19-00217.
[24] R. Leechaisit, R. Pingaew, V. Prachayasittikul, A. Worachartcheewan, S. Prachayasittikul, S. Ruchirawat, V. Prachayasittikul, Synthesis, molecular docking, and QSAR study of bis-sulfonamide derivatives as potential aromatase inhibitors, Bioorg. Med. Chem. 27 (2019) 115040, https://doi.org/10.1016/j.bmc.2019.08.001.
[25] A. Stefanachi, A.D. Favia, O. Nicolotti, F. Leonetti, L. Pisani, M. Catto, C. Zimmer, R.W. Hartmann, A. Carotti, Design, synthesis, and biological evaluation of imidazolyl derivatives of 4,7-disubstituted coumarins as aromatase inhibitors selective over 17-alpha-hydroxylase/C17-20 lyase, J. Med. Chem. 54 (2011) 1613–1625, https://doi.org/10.1021/jm101120u.
[26] R. Ghodsi, E. Azizi, M. Grazia Ferlin, V. Pezzi, A. Zarghi, Design, synthesis and biological evaluation of 4-(imidazolylmethyl)-2- aryl-quinoline derivatives as aromatase inhibitors and anti-breast cancer agents, Lett. Drug Des. Discov. 13 (2015) 89–97, https://doi.org/10.2174/1570180812666150611185605.
[27] M.G. Ferlin, D. Carta, R. Bortolozzi, R. Ghodsi, A. Chimento, V. Pezzi, S. Moro, N. Hanke, R.W. Hartmann, G. Basso, G. Viola, Design, synthesis, and structure-activity relationships of azolylmethylpyrroloquinolines as nonsteroidal aromatase inhibitors, J. Med. Chem. 56 (2013) 7536–7551, https://doi.org/10.1021/jm400377z.
[28] C. Chamduang, R. Pingaew, V. Prachayasittikul, S. Prachayasittikul, S. Ruchirawat, V. Prachayasittikul, Novel triazole-tetrahydroisoquinoline hybrids as human aromatase inhibitors, Bioorg. Chem. 93 (2019) 103327, https://doi.org/10.1016/j.bioorg.2019.103327.
[29] R. Pingaew, V. Prachayasittikul, P. Mandi, C. Nantasenamat, S. Prachayasittikul, S. Ruchirawat, V. Prachayasittikul, Synthesis and molecular docking of 1,2,3-triazole-based sulfonamides as aromatase inhibitors, Bioorg. Med. Chem. 23 (2015) 3472–3480, https://doi.org/10.1016/j.bmc.2015.04.036.
[30] Z. Sahin, M. Ertas, B. Berk, S.N. Biltekin, L. Yurttas, S. Demirayak, Studies on non-steroidal inhibitors of aromatase enzyme; 4-(aryl/heteroaryl)-2-(pyrimidin-2-yl)thiazole derivatives, Bioorg. Med. Chem. 26 (2018) 1986–1995, https://doi.org/10.1016/j.bmc.2018.02.048.
[31] A.S. Mayhoub, L. Marler, T.P. Kondratyuk, E.J. Park, J.M. Pezzuto, M. Cushman,

Optimization of thiazole analogues of resveratrol for induction of NAD(P)H: quinone reductase 1 (QR1), Bioorg. Med. Chem. 20 (2012) 7030–7039, https://doi.org/10.1016/j.bmc.2012.10.006.
[32] A. Andreani, A. Leoni, A. Locatelli, R. Morigi, M. Rambaldi, R. Cervellati, E. Greco, T.P. Kondratyuk, E.J. Park, K. Huang, R.B. van Breemen, J.M. Pezzuto, Chemopreventive and antioxidant activity of 6-substituted imidazo[2,1-b] thiazoles, Eur. J. Med. Chem. 68 (2013) 412–421, https://doi.org/10.1016/j.ejmech.2013.07.052.
[33] M. Ertas, Z. Sahin, B. Berk, L. Yurttas, S.N. Biltekin, S. Demirayak, Pyridine-substituted thiazolylphenol derivatives: synthesis, modeling studies, aromatase inhibition, and antiproliferative activity evaluation, Arch. Pharm. (Weinheim) 351 (2018), e1700272, https://doi.org/10.1002/ardp.201700272.
[34] D. Osmaniye, S. Gorgulu, B.N. Saglik, S. Levent, Y. Ozkay, Z.A. Kaplancikli, Design, synthesis, in vitro and in silico studies of some novel thiazole-dihydrofuran derivatives as aromatase inhibitors, Bioorg. Chem. 114 (2021) 105123, https://doi.org/10.1016/j.bioorg.2021.105123.
[35] C.S. Rosenfeld, D.A. Shay, V.J. Vieira-Potter, Cognitive effects of aromatase and possible role in memory disorders, Front. Endocrinol. 9 (2018) 610, https://doi.org/10.3389/fendo.2018.00610.
[36] M. Jatczak, K. Muylaert, L.M. De Coen, J. Keemink, B. Wuyts, P. Augustijns, C.V. Stevens, Straightforward entry to pyrido[2,3-d]pyrimidine-2,4(1H,3H)-diones and their ADME properties, Bioorg. Med. Chem. 22 (2014) 3947–3956, https://doi.org/10.1016/j.bmc.2014.06.009.
[37] R. Arif, M. Rana, S. Yasmeen, Amaduddin, M.S. Khan, M. Abid, M.S. Khan, Rahisuddin, Facile synthesis of chalcone derivatives as antibacterial agents: synthesis, DNA binding, molecular docking, DFT and antioxidant studies, J. Mol. Struct. 1208 (2020) 127905, https://doi.org/10.1016/j.molstruc.2020.127905.
[38] F.A. Khan, R.H. Patil, D.B. Shinde, J.N. Sangshetti, Bacterial Peptide deformylase inhibition of cyano substituted biaryl analogs: synthesis, in vitro biological evaluation, molecular docking study and in silico ADME prediction, Bioorg. Med. Chem. 24 (2016) 3456–3463, https://doi.org/10.1016/j.bmc.2016.05.051.
[39] Y. Isyaku, A. Uzairu, S. Uba, Computational studies of a series of 2-substituted phenyl-2-oxo-, 2-hydroxyl- and 2-acylloxyethylsulfonamides as potent anti-fungal agents, Heliyon 6 (2020), e03724, https://doi.org/10.1016/j.heliyon.2020.e03724.
[40] C.A. Lipinski, F. Lombardo, B.W. Dominy, P.J. Feeney, Experimental and computational approaches to estimate solubility and permeability in drug discovery and development settings, Adv. Drug Deliv. Rev. 23 (1997) 3–25, https://doi.org/10.1016/S0169-409x(96)00423-1.
[41] Schrödinger Release 2020, Desmond, Schrödinger, LLC, New York, NY, USA, 2020.
[42] S.S. Ahmad, M. Sinha, K. Ahmad, M. Khalid, I. Choi, Study of caspase 8 inhibition for the management of alzheimer's disease: a molecular docking and dynamics simulation, Molecules 25 (2020), https://doi.org/10.3390/molecules25092071.
[43] SwissADME, A free web tool to evaluate pharmacokinetics, drug-likeness and medicinal chemistry friendliness of small molecules, Sci. Rep. 7 (2017) 1–13.
[44] B. Kaya, L. Yurttas, B.N. Saglik, S. Levent, Y. Ozkay, Z.A. Kaplancikli, Novel 1-(2-pyrimidin-2-yl)piperazine derivatives as selective monoamine oxidase (MAO)-A inhibitors, J. Enzym. Inhib. Med. Chem. 32 (2017) 193–202, https://doi.org/10.1080/14756366.2016.1247054.
[45] D. Osmaniye, B.N. Sağlık, S. Levent, S. Ilgın, Y. Özkay, Z.A. Kaplancıklı, Design, synthesis, in vitro and in silico studies of some novel triazoles as anticancer agents for breast cancer, J. Mol. Struct. 1246 (2021) 131198, https://doi.org/10.1016/j.molstruc.2021.131198.
[46] B.N. Saglik, A.M. Sen, A.E. Evren, U.A. Cevik, D. Osmaniye, B. Kaya Cavusoglu, S. Levent, A.B. Karaduman, Y. Ozkay, Z.A. Kaplancikli, Synthesis, Investigation of Biological Effects and in Silico Studies of New Benzimidazole Derivatives as Aromatase Inhibitors, Z Naturforsch C J Biosci, 2020, https://doi.org/10.1515/znc-2020-0104.
[47] Schrödinger Release 2020-3, Maestro, Schrödinger, LLC, New York, NY, USA, 2020.
[48] Schrödinger Release. 2020-1: LigPrep 2020, Schrödinger, LLC, New York, NY, USA, 2020.
[49] Schrödinger Release 2020-3, Glide, Schrödinger, LLC, New York, NY, USA, 2020.
[50] ConfGen, Schrödinger Maestro, New York, 2020.
[51] N. Chirico, P. Gramatica, Real external predictivity of QSAR models: how to evaluate it? Comparison of different validation criteria and proposal of using the concordance correlation coefficient, J. Chem. Inf. Model. 51 (2011) 2320–2335, https://doi.org/10.1021/ci200211n.